Applied Clay Science 267 (2025) 107741

Contents lists available at ScienceDirect

Applied Clay Science

journal homepage: www.elsevier.com/locate/clay

Research Paper

Synergistic effect of processing water treatment sludge rich in kaolinite for the sustainable production of LC^3

Tacila Bertulino [a,*], Fernanda W.C. Araújo [b], Antônio A. Melo Neto [a]

[a] Laboratory of Binder Technology (LabTag), Department of Civil and Environmental Engineering, Federal University of Pernambuco, Recife, Brazil
[b] Department of Rural Technology, Federal Rural University of Pernambuco, Recife, Pernambuco, Brazil

ARTICLE INFO

Keywords:
Water treatment sludge ash
Pozzolanic reactions
LC^3, Box-Behnken
High-reactivity pozzolan

ABSTRACT

The increasing population and urban development intensify the need for potable water, resulting in higher production of sludge in water treatment plants (WTPs). To mitigate the improper disposal of sludge and reduce carbon dioxide emissions from Portland cement production, the pozzolanic activity of sludge and its ashes, derived from WTPs and referred to as WTPA, is being investigated. These materials are being evaluated as supplementary cementitious materials (SCMs), enabling their application in the development of limestone calcined clay cement (LC^3). The WTPA samples calcined at 600, 700, and 800 °C were analyzed using X-ray fluorescence (XRF), X-ray diffraction (XRD), thermogravimetric analysis (TGA), scanning electron microscopy (SEM), Brunauer-Emmett-Teller (BET) surface area analysis, Blaine fineness, and laser diffraction techniques. Compressive strength, electrical conductivity, and R^3 tests were performed to evaluate pozzolanic reactivity of WTPA. The influence of calcination temperature, the proportion of WTPA, and the water/cement ratio were studied using the Box-Behnken design in LC^3 mixtures. The results suggest that the calcination temperature of 700 °C is ideal for producing pozzolana, standing out with an SAI of 140 % and 19.09 MPa in the lime test. This temperature also favored a higher combined water content (15.8 g/100 g of paste), indicative of resistant hydrated compounds. Additionally, the multi-objective analysis indicated that the optimal formulation for WTPA use in LC^3 involves a calcination temperature around 700 °C, a replacement rate of 17.62 %, and a water/cement ratio of 0.54. This formulation provides a fluid consistency, while compressive strength reaches 35.57 MPa, demonstrating the effectiveness of sludge as pozzolana. This study provides new insights into the use of water treatment plant sludge ash as a sustainable material for the development of LC^3, offering a promising alternative to reduce the environmental impact of the cement industry.

1. Introduction

Water treatment plants (WTPs) generate sludge as a byproduct of coagulation, flocculation, sedimentation, and filtration processes (Hoppen et al., 2005; Achon and Cordeiro, 2015; Ahmad et al., 2016c). Projections estimate a 20–30 % increase in water demand, reaching between 5500 and 6000 km^3 annually by 2050 (Burek et al., 2016), which may intensify sludge production. This sludge can account for 0.1 % to 3 % of the treated water volume daily, resulting in annual production reaching up to 180 km^3, depending on treatment efficiency (Di Bernardo et al., 2012). Approximately 22 % of this sludge is sent to landfills, while 56 % is discharged into water bodies (IBGE, 2017; de Carvalho Gomes et al., 2019). Although incineration is effective in reducing volume, it is costly, reaching up to US$ 329.00 per ton, and requires strict environmental controls due to pollutant emissions (Januário and Ferreira Filho, 2002; Hendges et al., 2017). Given the challenges associated with sludge disposal and treatment, the search for more sustainable solutions has intensified.

The ashes from WTPs exhibit promising chemical characteristics that make them suitable as supplementary cementitious materials (SCMs). Their composition is rich in Al_2O_3, Fe_2O_3, and SiO_2, and they also contain particles of sand, clay, and coagulants such as aluminum salts and iron ions (Sales et al., 2011; Huang and Wang, 2013; Pinheiro et al., 2014; Ahmad et al., 2016a, 2016b; de Oliveira Andrade, 2018). The similarity to the components of Portland cement and pozzolanic materials enables their use in the cement industry, especially after calcination at temperatures between 600 and 700 °C, which activates their pozzolanic reactivity (Gastaldini et al., 2015; Hagemann et al., 2019). Furthermore,

* Corresponding author.
E-mail address: tacila.bertulino@ufpe.br (T. Bertulino).

https://doi.org/10.1016/j.clay.2025.107741
Received 2 September 2024; Received in revised form 19 January 2025; Accepted 31 January 2025
0169-1317/© 2025 Elsevier B.V. All rights are reserved, including those for text and data mining, AI training, and similar technologies.

WTP ashes can reduce clinker consumption, contributing to the mitigation of CO_2 emissions (Cembureau, 2013; Gartner and Hirao, 2015; GCCA, 2019). The partial substitution of raw materials with industrial waste and by-products is becoming established as a viable and sustainable strategy for the cement industry, as highlighted in several studies (Schneider et al., 2011; Scrivener et al., 2018a, 2018b; Zhang et al., 2024; Yu et al., 2023a, 2023b).

Since 1994, there have been attempts to incorporate WTPs into cement compositions, initially by combining sludge with limestone to form the clinker raw mix (Tay and Show, 1994). However, the mechanical performance was not satisfactory. Research into the feasibility of using artificial pozzolans gained prominence in the late 20th century, as evidenced by a 1997 study that explored the viability of pozzolans obtained by calcining sewage sludge (Morales, 1997). Hagemann et al. (2019) examined the reaction of WTP in concrete, replacing up to 30 % of WTP ash and 15 % of limestone with Portland cement, resulting in savings of up to 38.4 %. More recently, Ruviaro and Silvestro (2023) investigated the feasibility of using WTP ashes (0–30 %) and eggshells (0–15 %) as substitutes for clay and limestone, observing an approximate 10 % reduction in compressive strength at 91 days but a 41 % reduction in CO_2 emissions.

In this context, limestone calcined clay cement (LC^3) is a ternary blend composed of Portland cement, calcined clay, and limestone (Blouch et al., 2023; Bonavetti et al., 2022). This innovative solution offers significant environmental benefits compared to ordinary Portland cement (OPC). LC^3 can achieve a potential 50 % reduction in Portland cement usage, cutting CO_2 emissions by 30 to 40 %, while maintaining or even improving the mechanical properties and durability of cement (Antoni et al., 2012; Bishnoi et al., 2014; Scrivener, 2014; Sánchez Berriel et al., 2016; Avet, 2017; Scrivener et al., 2018a, 2018b).

This article aims to contribute to the international database by analyzing WTP and evaluating its performance after thermal treatment and grinding, in combination with LC^3. Unlike previous studies, which focused on incorporating WTPs as a direct substitute for Portland cement or as a complete replacement for calcined clay, this research explores the substitution of calcined clay with WTP ash at different levels, creating a quaternary blend. Additionally, the study compares the performance of WTP with other SCMs and conducts pozzolanicity tests to investigate its reactivity, providing a detailed assessment of its potential as a component in the formulation of sustainable cements. By optimizing the LC^3 formulation with this approach, the study seeks to expand knowledge about the technical and environmental feasibility of using WTPs and contribute to the development of more sustainable solutions in the construction industry.

2. Materials and methods

2.1. Materials

2.1.1. Water treatment sludge

The sludge used in this study was collected from the Pirapama Water Treatment Station in Recife, Pernambuco, Brazil—the state's largest water supply system with a production capacity of 5.13 m^3/s and generating 93 tons of sludge daily. Approximately 90 % of the sludge originates from the decantation system. The sludge for this study was collected from the stabilization pond in its liquid form and transferred to an outdoor drying area for seven days. Afterward, it was dried in an oven at 100 °C for 24 h and then allowed to cool naturally. The dried sludge was then disaggregated using a ball mill for one hour and was designated as water sludge at 100 °C (WS100).

The calcination temperatures were determined based on prior research, varying between 600 and 800 °C (Gastaldini et al., 2015; Hagemann, 2018; Hagemann et al., 2019; Agra, 2022; Agra et al., 2023; Ruviaro and Silvestro, 2023; Koutsouradi et al., 2025), temperatures below 550 °C may contain organic matter, while 800 °C is the upper limit for maintaining pozzolanic properties. The ash was labeled as WA600, WA700, and WA800 based on the calcination temperature. Each sample was heated in a Linn High Therm KK 260 electric oven at a rate of 10 °C/min until reaching the target temperatures of 600, 700, and 800 °C, respectively. The temperature was then maintained for 180 min before cooling to room temperature.

Post-calcination, the ash turned a reddish hue and was ground for one hour to standardize the composition and reduce particle sizes, thereby enhancing their pozzolanic potential. Figs. 1 and 2 illustrate the final samples and the process flowchart for sample preparation.

2.1.2. Other materials

The LC^3 composition utilized high early strength Portland cement (CPV ARI - similar to ASTM type III cement) from Cimento Nacional. The clay used, sourced from Votorantim Cimentos and used in commercial pozzolanic cement formulations, consists of 40 % black clay and 60 % yellow clay. This natural clay was dried for 24 h in an oven and then calcined at 800 °C for 1 h to ensure complete calcination and pozzolanic reactivity (Fernandez et al., 2011; Scrivener et al., 2018a, 2018b; Liu et al., 2021; Zolfagharnasab et al., 2021; Zunino and Scrivener, 2021; Bahman-Zadeh et al., 2022; Yadak Yaraghi et al., 2022).

For the LC^3 mix, 30 % of the Portland cement was replaced with calcined clay and 15 % with limestone, maintaining an ideal 2:1 ratio between the two (Antoni, 2013; Scrivener et al., 2018a, 2018b). Additionally, 5 % of the cement was replaced with calcium sulfate dihydrate ($CaSO_4 \cdot 2H_2O$) of 98 % analytical purity to ensure proper cement sulfation of the cement, following typical LC^3 formulations. It is important to note that, in this study, commercial OPC. was used instead of clinker.

To evaluate the pozzolanic potential of WTP sludge, its compressive strength performance was compared with two other traditionally used commercial pozzolans, metakaolin (MK) and fly ash (FA). For the pozzolanic activity test with calcium hydroxide and the electrical conductivity test, calcium hydroxide PA ($Ca(OH)_2$) of 95 % minimum purity was used, as specified by NBR 5751 (ABNT NBR 5751, 2015). The fine aggregate was quartz sand with a maximum particle size of 2.36 mm, a specific mass of 2.65 g/cm^3, and a fineness modulus of 2.33. Table 1 details the chemical and physical properties of these materials, using the same parameters for characterizing WTP sludge.

2.2. Characterization of WTP

The chemical composition and microstructure of the samples were evaluated using X-ray fluorescence (XRF) with semiquantitative analysis on pressed pellets using the Rigaku ZSX Primus II spectrometer. Sludge particle analysis was performed using a TESCAN Mira3-LM scanning electron microscope (SEM) with a field emission gun (FEG), focusing on topographical regions via scattered electron signals (SE).

For physical characterization, density was measured with a Le Chatelier flask (ABNT NM23, 2000). The specific surface area was determined using the Blaine method (ABNT NBR 5751, 2015), while the BET method via nitrogen sorption on a Micromeritics ASAP 2420 was used for detailed surface area analysis. Prior to analysis, the samples were degassed at 373 K for 12 h in the degassing port. Particle size distribution was analyzed by laser diffraction with a Malvern Mastersizer 2000 equipped with the Hydro 2000MU dispersion unit, covering a range of 0.02 to 2000 μm.

Mineralogical phases of the pastes were identified through X-ray diffraction (XRD) on a Bruker PHASER D2 diffractometer, scanning from 5 to 80°2θ with 0.05°2θ increments and a 0.575 s/step count time. CuKα radiation at 20 mA and 40 kV was used, with compound identification supported by X'pert Highscore Plus software and the ICDD database. Thermogravimetric analysis (TGA) was performed with a Netzsch STA 2500 at a 10 °C/min heating rate up to 1000 °C in a nitrogen atmosphere at 40 ml/min.

TGA quantifies the kaolinite content in raw sludge using the tangent method (Scrivener et al., 2016). Kaolinite dehydroxylation occurs between 400 and 600 °C (Fernandez et al., 2011; Ptáček et al., 2014; Avet

Fig. 1. From left to right: the appearance of the WS100, WA600, WA700 and WA800 treatment sludge after machining.

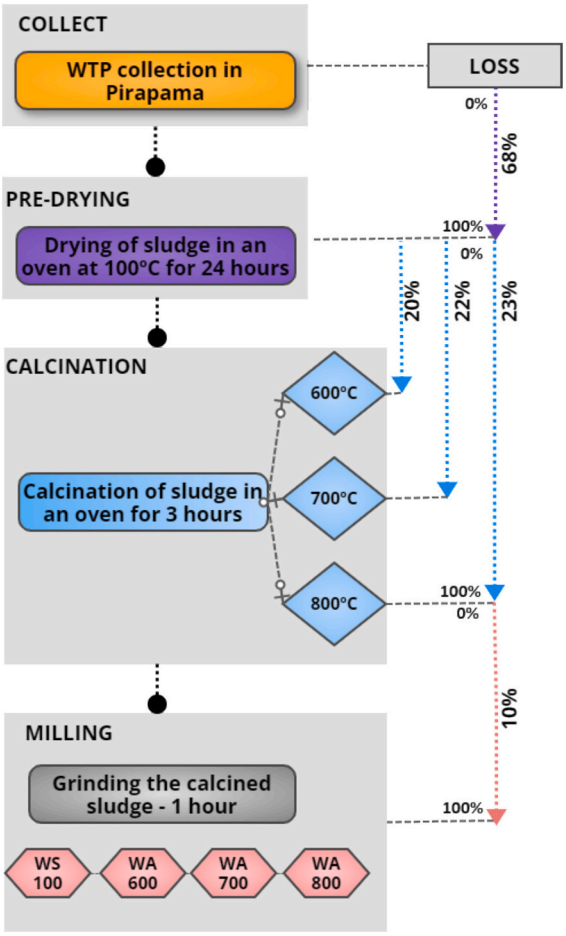

Fig. 2. Schematic flowchart of the water sludge ash preparation procedure and losses in each process.

and Scrivener, 2018). The kaolinite content is calculated from the mass loss during dehydroxylation, relating to the molar masses of kaolinite (258.16 g/mol) and water (18 g/mol), as shown in Eq. 1.

$$\text{Kaolinite}\ (\%) = \text{Wt}_{\text{kaolinite}}\ \text{x}\ \frac{M_{kaolinite}}{2.M_{H_2O}} \tag{1}$$

2.3. Assessment of pozzolanic activity

Pozzolanic activity was evaluated through four tests: two for compressive strength, one for electrical conductivity, and one for combined water content, as summarized in Table 2.

In the first test, according to Brazilian standard NBR 5751 (ABNT NBR 5751, 2015), three cylindrical specimens (50 × 100 mm) were prepared with 104 g of analytical-grade calcium hydroxide. The mass of the pozzolanic material (m) was set as twice the volume of calcium hydroxide, with the ratio given by Eq. 2, where δ_{poz} represents the specific mass of the pozzolanic material and δ_{CH} is the specific mass of calcium hydroxide. In preparing the mortar, the binder-to-sand ratio was 1:3 by mass, adjusting the water to a consistency index of (165 ± 5) mm according to NBR 7215 (ABNT NBR 7215, 2019). A superplasticizer was used to set the water-to-binder ratio (w/b) at 0.80. The specimens were cured in metal molds for seven days: one day at room temperature and six days at (55 ± 2)°C. To be considered pozzolanic, the compressive strength must exceed 6 MPa, as per NBR 12653 (ABNT NBR 5752, 2014).

$$\mathbf{m} = 2.\left(\frac{\delta_{poz}}{\delta_{CH}}\right).104g \tag{2}$$

In the second test, the Strength Activity Index (SAI) was determined with Portland cement at 28 days, following the NBR 5752:2014 standard. Six cylindrical specimens (50 × 100 mm) were molded with one part binder to three parts sand and a w/b ratio of 0.48. The mortars, composed of 75 % cement and 25 % pozzolan, were cured in a saturated lime solution until the test at 28 days. The SAI was calculated as the ratio between the average strength of samples containing only Portland cement and pozzolanic material and the average strength of samples containing only Portland cement (Table 3).

The pozzolanic activity of the WTP was evaluated by electrical conductivity, following the model by Paya et al. (2001) adapted by Basto et al. (2019). The 1000-s test involved heating 1050 ml of water, adding 840 mg of $Ca(OH)_2$ at 60 ± 1 °C, stirring at 700 rpm for 1 h, transferring 200 ml to a beaker, and adding 4 g of pozzolan. Conductivity measurements were taken with a Digimed DM-32 v.2.0 and DMC-001 XTX cell, with data collected every second by a Raspberry Pi 3. The corrected electrical conductivity (C_{poza}) was calculated by the difference between the conductivity of the solution with $Ca(OH)_2$ + pozzolan (C_{pozCH}) and the conductivity of a solution with only pozzolan (C_{poz}), as shown in Eq. 3. The loss of conductivity (%LC_t) was determined by the ratio between the initial difference (C_0) and the corrected electrical conductivity, as given by Eq. 4.

$$C_{poza} = C_{pozCH} - C_{poz} \tag{3}$$

$$(\%\mathbf{LCt}) = \left(\frac{C_o - C_{poza}}{C_o}\right)*100 \tag{4}$$

The rapid, robust, and relevant chemical reactivity test (R^3) was performed according to American Standard C1897 (ASTM, 2020). This method assesses the reactivity of supplementary cementitious materials, including calcium hydroxide (30 g), calcium carbonate (5 g), SCM (10 g), and potassium solution (liquid/solids ratio of 1.2 by mass). The mixture was stirred at 1600 rpm for 2 min and cured at 40 °C for 7 days. The chemically combined water content was measured in a Timer One Plus VRC muffle furnace at 350 °C. After cooling in a desiccator, the mass of the empty crucible (w_c) was recorded, and 5 ± 0.5 g of crushed paste (w_o) was transferred. The total mass (w_h) was recorded after heating and cooling. The chemically combined water content (Eq. 5) was calculated in g per 100 g of dry paste at 40 °C.

$$\boldsymbol{H_2O_{Combined.dry}} = \frac{w_o - w_h}{w_o - w_c}\ x\ 100 \tag{5}$$

Table 1
Physical and chemical properties of materials.

Materials	Cement	Clay	Calcined clay	Limestone	Calcium hydroxide	Metakaolin	Fly ash
SiO_2	15.58	42.33	46.12	1.25	0.26	59.30	55.12
Al_2O_3	4.74	14.89	14.66	0.61	0.10	33.37	32.16
Fe_2O_3	2.67	4.51	5.29	0.30	0.08	1.45	3.72
CaO	60.14	14.37	17.03	44.25	72.98	0.08	1.38
MgO	1.62	1.61	2.35	8.50	0.96	0.21	0.80
SO_3	5.06	1.41	2.01	0.18	0.04	0.05	0.48
K_2O	1.32	2.99	3.60	0.09	0.24	0.27	2.81
N_2O	0.19	0.16	0.16	–	–	–	–
P_2O_5	0.67	0.13	0.15	0.04	0.07	0.04	0.10
LOI*	7.46	16.54	7.45	44.56	25.13	3.87	2.15
Density (g/cm^3)	3.08	2.59	2.66	2.74	2.22	2.61	2.04
BET (g/cm^3)	1.35				8		1.06
Blaine (m^2/g)	453.00	452.90	770.88	331.68	1597.80	698.00	319.00
D_{50} (μm)	16.05	7.47	12.81	45.95			
$D_{4,3}$ (μm)	22.38	14.61	17.43	100.25			

– not determined.
* Loss on ignition at 1000 °C.

Table 2
Summary of experiments to verify the pozzolanicity of water treatment plant sludge.

Test	System	Standard	Healing condition	Age	Analyzed parameter
Pozzolanic activity with lime	$Ca(OH)_2$ + SCM mortar	ABNT NBR 5751	Sealed 24 h at 23 °C and then 55 °C	7 days	• Compressive strength
Strength Activity Index (SAI)	Cementitious mortar	ABNT NBR 5752	Immersed, 23 °C	28 days	• Compressive strength
Electrical Conductivity	Solution of $Ca(OH)_2$ + SCM	Paya et al. (2001) e Basto et al. (2019)	–	During 1000 s	• Loss of conductivity
R^3	Mass of $Ca(OH)_2$ + SCM + $CaCO_3$	ASTM C1897	Thermal, 40 °C	7 days	• Chemically bound water

Table 3
Quantity of material, by mass (g), used for testing compressive strength.

	Testing compressive strength tests with lime (NBR 5751).						
Reference	Type	Lime (g)	Pozzolan (g)	Water (g)	SP (g)	Sand (g)	Ic (mm)
WS100	WS100	104	228.61	266.09	16.63	936	230.00
WA600	WA600	104	249.23	282.58	17.66	936	223.00
WA700	WA700	104	255.78	287.83	17.99	936	220.00
WA800	WA800	104	262.34	293.07	18.32	936	221.00
CL	Clay	104	242.67	277.33	17.33	936	290.00
CC	Calcined clay	104	249.23	282.58	17.66	936	280.00
LS	Limestone	104	256.72	288.58	18.04	936	291.00
MK	Metakaolin	104	244.54	278.83	17.43	936	240.00
FA	Fly ash	104	191.14	236.11	14.76	936	250.00

	Testing compressive strength at 28 days (NBR 5752)						
Reference	Type	Cement (g)	Pozzolan (g)	Water (g)	SP (g)	Sand (g)	Ic (mm)
CP	Cement	624	0	300	–	1872	165.00
WS100	WS100	468	156	300	12.48	1872	159.00
WA600	WA600	468	156	300	22.50	1872	155.00
WA700	WA700	468	156	300	19.53	1872	162.50
WA800	WA800	468	156	300	19.53	1872	163.00
CL	Clay	468	156	300	7.45	1872	165.00
CC	Calcined clay	468	156	300	5.49	1872	155.00
LS	Limestone	468	156	300	–	1872	165.00
MK	Metakaolin	468	156	300	8.58	1872	175.00
FA	Fly ash	468	156	300	–	1872	162.50

2.4. Response surface design

To evaluate the compressive strength and consistency index of LC^3 mortars, a response surface design (RSD) was used. The aim is to optimize the use of WTPA in LC^3 cement, enhancing its application as a supplementary cementitious material and identifying key variables in sludge preparation that affect the quaternary mix design.

Response surface methodology (RSM) is employed to determine the optimal region of independent variables (Ray and Lalman, 2011). While full factorial design (FFD) is often impractical due to the high number of experiments, central composite design (CCD) and Box-Behnken design (BBD) are more feasible (Box et al., 1978; Myer and Montogomery, 2002; Bae and Shoda, 2005). For quadratic response surface models with three or more factors, BBD is preferred due to its efficiency in exploring

the design space (Myer and Montogomery, 2002; Ray, 2006; Ray et al., 2009).

BBD limits the range of factors to −1, 0, and 1, representing the lowest, middle, and highest values of the actual factors, respectively. This ensures that factor variations stay within safe limits. For a BBD with three factors, the number of experiments (n) is given by $n = 2\times(x - 1) + C_0$, where x is the number of factors and C_0 is the number of central points (Ray and Lalman, 2011). In this study, BBD was used to examine the effects of WTPA calcination temperature, WTPA content (replacing calcined clay), and water/binder ratio in LC^3 mortar, with three factors and three central points, resulting in a total of 15 experiments (Table 4).

The LC^3 formulation consists of 50 % cement, 30 % calcined clay, 15 % limestone, and 5 % gypsum. Replacements of calcined clay with WTPA (5 %, 52.5 %, and 100 %) were tested, covering the full range of calcined clay applications in LC^3. Mortar molding, curing, and compressive strength testing followed EN 196:2016, with tests conducted at 28 days using six cubic specimens per experiment. The consistency index was assessed according to NBR 13276 (ABNT NBR 13276, 2016) and is similar to the American standard C1437–20 (ASTM C1437, 2020). The additive content was kept at 4 % of the binder mass across all mixtures. Data analysis was performed using Minitab Statistical Software version 21.4.2.

3. Results and discussion

3.1. Chemical and microstructural characteristics of WTP

Chemical compounds in cement and ash, even in small quantities, influence hydration, workability, and strength, impacting the resulting binder's characteristics (Krejcirikova et al., 2019). Table 5 highlights elemental oxide concentrations for dry and calcined ash, including essential SiO_2 and Al_2O_3. Amorphous siliceous or siliceous-aluminous materials react with calcium hydroxide at room temperature, forming cementitious compounds. Pozzolanic activity is linked to chemical composition (Malhotra and Mehta, 1996). According to Brazilian standard NBR 12653 (ABNT NBR 12653, 2014), criteria include minimum levels of $SiO_2 + Al_2O_3 + Fe_2O_3 \geq 70$ %, $SO_3 < 4$ %, loss on ignition <10 %, and alkalis in $Na_2O < 1.5$ %. WTP samples meet these parameters, except WS100, which exceeds the fire loss limit.

Table 5
Chemical composition of WTP and ash.

Oxides	WS100	WA600	WA700	WA800
SiO_2	32.61	38.50	40.55	40.78
Al_2O_3	30.33	38.72	40.20	40.29
P_2O_5	0.32	0.35	0.29	0.34
SO_3	0.34	0.48	0.15	0.55
Cl	-.	–	0.01	0.04
K_2O	0.25	0.29	0.33	0.31
N_2O	0.05	0.05	0.18	0.07
CaO	0.09	0.29	0.25	0.48
MnO	0.04	N.D.	N.D.	N.D.
Fe_2O_3	10.47	12.86	12.21	12.69
TiO_2	1.38	1.73	0.92	0.99
MgO	0.16	0.15	0.25	0.23
SrO	–	–	–	–
CuO	–	–	–	–
$SiO_2 + Al_2O_3 + Fe_2O_3$	73.41	90.08	92.96	93.76
LOI*	24.52	7.31	4.55	3.15

–not determined.
* Loss in ignition at 1000 °C.

The oxide composition of WTP samples aligns with literature (Pinheiro et al., 2014; de Oliveira Andrade et al., 2018; de Carvalho Gomes et al., 2019; Santos et al., 2019; Bohórquez González et al., 2020), notably in Al_2O_3 content due to aluminum sulfate use in water treatment. The samples show low alkaline content, especially Na_2O and K_2O (< 0.6 %), which is critical since these oxides can compromise the pozzolanic reaction by interacting with cement hydration products (Berenguer et al., 2021). The loss on ignition in the sludge results from the dehydroxylation of phyllosilicates and decarbonation of carbonates (Monteiro et al., 2008; Rodríguez et al., 2010; Owaid et al., 2014), in addition to the combustion of organic matter, as mentioned earlier.

Section 2 of the supplementary material shows SEM and EDX analysis of WTP particles and the calcined material. In dry sludge (WS100), particles vary in size and shape. Post-calcination, they transition to more rounded shapes, indicating a less crystalline structure. Rodríguez et al. (2010) noted incineration results in spherical particles, often with laminar or annular structures. EDX confirmed the predominance of

Table 4
Summary of real and coded variables from the experimental matrix.

	Variable code		
Experimental levels	Calcination temperature	WTPA content [a]	w/b ratio [b]
Low (−1)	600 °C	5 %	0.40
Medium (0)	700 °C	52.5 %	0.50
High (1)	800 °C	100 %	0.60

	Mixture content in grams (g)										
N	Pattern	°C	Content	w/b	Cement	Calcined clay	Limestone	Gypsum	WTPA	w/b	Sand
1	"–0"	−1	−1	0	150	85.5	45	15	4.5	150	900
2	"+ – 0"	1	−1	0	150	85.5	45	15	4.5	150	900
3	"– + 0"	−1	1	0	150	0	45	15	90	150	900
4	"++0"	1	1	0	150	0	45	15	90	150	900
5	"-0-"	−1	0	−1	150	45	45	15	47.25	120	900
6	"+0-"	1	0	−1	150	45	45	15	47.25	120	900
7	"-0+"	−1	0	1	150	45	45	15	47.25	180	900
8	"+0+"	1	0	1	150	45	45	15	47.25	180	900
9	"0–"	0	−1	−1	150	85.5	45	15	4.5	120	900
10	"0 + –"	0	1	−1	150	0	45	15	90	120	900
11	"0 – +"	0	−1	1	150	85.5	45	15	4.5	180	900
12	"0++"	0	1	1	150	0	45	15	90	180	900
13	"000"	0	0	0	150	45	45	15	47.25	150	900
14	"000"	0	0	0	150	45	45	15	47.25	150	900
15	"000"	0	0	0	150	45	45	15	47.25	150	900

[a] Substitution about the total content of calcined clay (90 g).
[b] Regarding the binder content (300 g).

silicon, aluminum, iron, and calcium, consistent with XRF results.

3.2. Physical characterization of WTP

In addition to pozzolanicity, the physical characteristics of the constituent materials also enhance the resistance of cementitious systems, such as particle size, shape, and texture (Goldman and Bentur, 1994). Table 6 presents data on specific mass, Blaine fineness, BET, and characteristic diameters ($D_{4,3}$, $D_{3,2}$, d_{10}, d_{50}, and d_{90}) obtained in the laser granulometry test.

The specific mass of the ash increases significantly after calcination due to the removal of organic matter from the sludge. The specific surface area measured by the Blaine method did not detect any variation in post-calcination fineness, remaining around 1990 m^2/kg. This method has limitations as it assumes air permeability in a uniform bed with regular particles, ignoring small pores (Grabowski and Wilanowicz, 2010; Arvaniti et al., 2015a; Safonov et al., 2021). For particles of varied sizes and high fineness, like SCMs, the BET method is more appropriate (Arvaniti et al., 2015b; Alderete et al., 2016; Abazarpoor and Halali, 2017).

The BET test identified that fineness decreased with increasing temperature, due to particle agglomeration and synthesis, making the ash harder and more resistant to grinding (Rashad, 2013; Souri et al., 2015). Section 2 of the supplementary material shows the particle size distribution of water sludge obtained by laser diffraction. The average diameters in Table 6 indicate that sludge calcination resulted in a slight increase in particle size (d_{50}), which is consistent with the reduction in specific surface area observed in the BET results after calcination.

3.3. Mineralogical and thermogravimetric analysis

Fig. 3 shows the diffractogram of WTP before and after calcination. In the raw dry sludge (WS100), prominent peaks of kaolinite ($Al_2Si_2O_5(OH)_4$), quartz (SiO_2), hematite (Fe_2O_3), and cristobalite (SiO_2) are observed. Kaolinite, a common clay mineral, suggests pozzolanic activity, though its reactivity needs to be induced by calcination (Avet, 2017; Briki, 2020; El Housseini, 2022). Calcination causes kaolinite dehydroxylation, forming metakaolin ($Al_2Si_2O_5(OH)_4 \longrightarrow Al_2Si_2O_5 + 2H_2O$) (Shvarzman et al., 2003; Arikan et al., 2009; Skibsted and Snellings, 2019), but this phase is not visible in the XRD (Altheman et al., 2023).

In the calcined samples (WA600, WA700, WA800), the absence of kaolinite peaks confirms dehydroxylation, evidenced by an amorphous halo between 20 and 30° (2θ), reinforcing the presence of amorphism in pozzolanic materials (Filho et al., 2017; Amaral et al., 2021). This absence aligns with previous studies (Hagemann, 2018; Ruviaro et al., 2021; Haustein et al., 2022; Agra et al., 2023).

The presence of iron in the calcined samples causes the reddish residue (Fig. 1) due to hematite oxidation (Nikolov and Karamanov, 2022), similar to commercial metakaolin (Medina, 2011; Altheman et al., 2017). Well-defined quartz and hematite peaks indicate a change in crystal structure at 800 °C, where higher calcination temperatures promote crystallization of amorphous silica, reducing pozzolanic activity (Fontes et al., 2003; Basto et al., 2019).

Section 2 of the supplementary material shows the TGA of dry raw sludge, with the derivative curve revealing peaks corresponding to heating phenomena. The first peak (30–110 °C) indicates evaporation of free and/or adsorbed water, with a 2.16 % mass loss. The second peak (180–360 °C) is due to oxidation of organic compounds, with a 6.13 % mass loss. A third peak (400–600 °C) indicates kaolinite dehydroxylation, with a 9.79 % mass loss. The final peak (850–950 °C), with a 1.35 % mass loss, is linked to the material's recrystallization. TGA quantified the kaolinite content at 70.17 %, characterizing WTP as high-quality clay, with kaolinite content exceeding 40 % (Mathieu Antoni, 2013; Avet, 2017; Scrivener et al., 2018a, 2018b).

3.4. Pozzolanic activity with lime

The compressive strength results of mortars containing lime and different SCMs are presented in Fig. 4. The blue line represents the minimum compressive strength limit established by NBR 12653 (ABNT NBR 5751, 2015). The figure shows that dry sludge, raw clay (CL) and limestone (LS) did not reach pozzolanic activity in the first 7 days. This occurrence was anticipated, as materials rich in kaolinite (WS100 and CL) only reach reactivity after thermal activation.

Limestone's effects are partially physical and chemical (Heikal et al., 2000; Lawrence et al., 2003). From a chemical perspective, there is a reaction between limestone and the aluminate phase, resulting in the formation of carboaluminate (Taylor, 1997). However, in tests containing only calcium hydroxide, limestone does not contribute silica-alumina to the pozzolanic equation, and the resulting paste does not provide aluminate for the formation of mono and hemicarboaluminate (Kakali et al., 2000; Bonavetti et al., 2001; Matschei et al., 2007; Lothenbach et al., 2008). This analysis confirms the conclusion that NBR 5751 (ABNT NBR 16372, 2015) constitutes an indirect test of pozzolanicity, emphasizing the importance of chemical interaction.

On the other hand, incinerated water sludge demonstrated a remarkable impact on lime tests, regardless of the calcination temperature. Even under the lowest calcination temperature, it recorded more than double the required strength, surpassing the expectations established for commercial pozzolans such as metakaolin (MK) and fly ash (FA).

3.5. Strength activity index

The pozzolanic potential with Portland cement is evaluated through axial compressive strength testing, following NBR 5752 (ABNT NBR 12653, 2014), using 25 % pozzolanic material fractions. The Pozzolanic Activity Index (SAI), calculated at 28 days according to NBR 12653 (ABNT NBR 12653, 2014), requires an SAI of at least 90 % of the reference value to consider the material pozzolanic.

The reference mortar, without pozzolanic material, reached a compressive strength of 28.06 MPa at 28 days. Fig. 5 shows the pozzolanicity index compared to this mortar. Similar results were observed in tests with Portland cement and calcium hydroxide mortars, where untreated samples (WS100 and CL) and LS did not meet the minimum requirement. WS100 and CL might be inert, possibly showing a 25 % reduction in strength due to dilution effects. Factors such as permeability, hydration kinetics, and porosity also influence strength development (Donatello et al., 2010a), and these samples contained high carbonaceous material.

WTPA samples showed SAI values of 89 %, 140 %, and 139 % for WA600, WA700, and WA800, respectively. Previous studies reported SAI ranging from 89 % to 112 % for this temperature range (Hagemann

Table 6
Physical characterization of dry and calcined sludge.

Material	Specific mass (g/cm^3)	Blaine (m^2/kg)	BET (m^2/g)	$D_{4,3}$	$D_{3,2}$	d_{10}(μm)	d_{50}(μm)	d_{90}(μm)
WS100	2.44	1089.62	51.09	36.32	9.72	3.45	22.47	74.47
WA600	2.66	1999.68	53.00	33.77	12.06	4.59	25.48	74.01
WA700	2.73	1990.20	51.95	36.54	12.88	4.97	27.46	82.26
WA800	2.80	1987.96	46.16	37.12	12.98	5.02	28.28	82.96

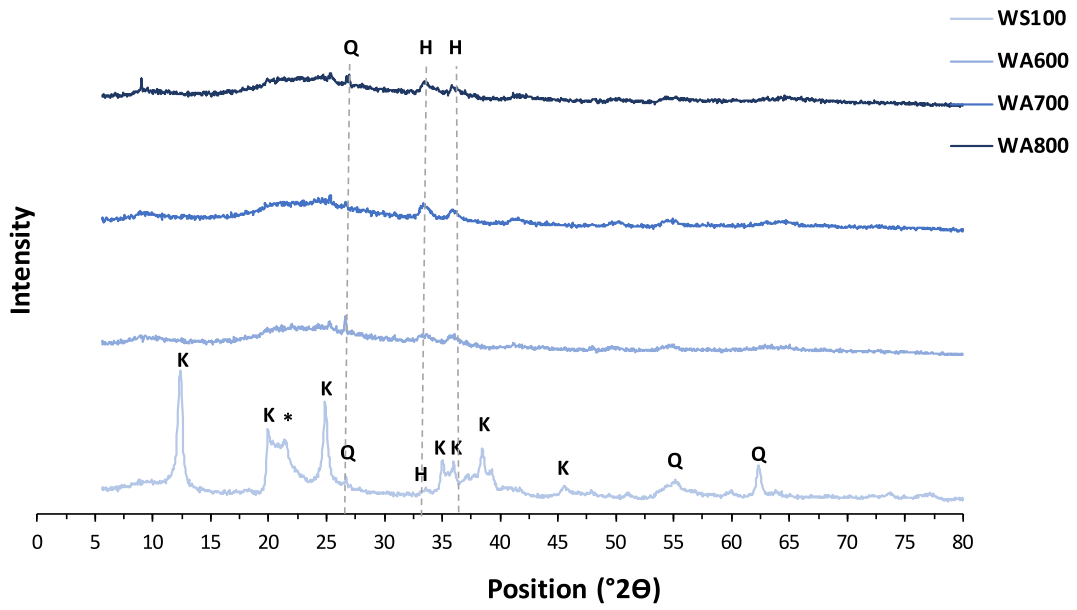

Fig. 3. WTP diffraction diagram, showing the presence of phases identified as quartz (Q), kaolinite (K), hematite (H), and cristobalite (*).

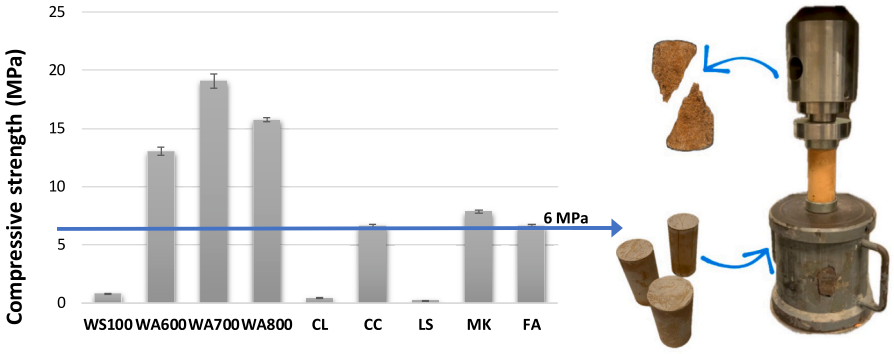

Fig. 4. Compressive strength results at 7 days for mortars with hydrated lime, representing standard deviation by error bars.

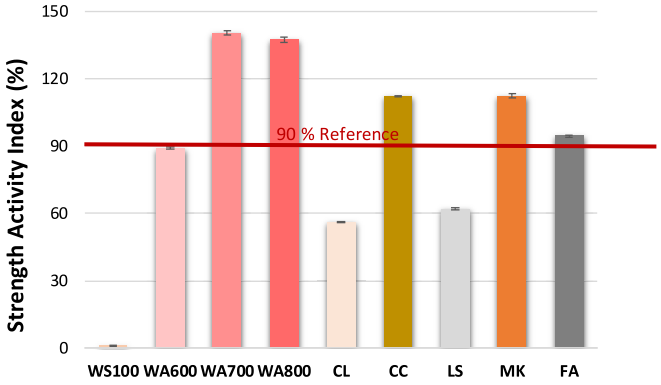

Fig. 5. Pozzolanic activity index at 28 days for mortars with 75 % cement and 25 % pozzolan by mass, with error bars indicating the standard deviation from the mean.

et al., 2019; Agra et al., 2023; Altheman et al., 2023). In the case of WA600, with an SAI below 90 %, this result aligns with previous physical analyses, and as pointed out by Agra et al. (2023), the high specific surface area of the material negatively impacted consistency, resulting in less efficient compaction in the fresh state compared to the samples calcined at 700 °C (WA700) and 800 °C (WA800). Additionally, Brazilian criteria are stricter than international standards such as ASTM C618–19 (ASTM, 2019) and BS 3892–1 (BS, 1997), which allow a 20 % pozzolan replacement with SAI requirements of over 80 % and 75 %, respectively, after 28 days.

The commercial pozzolans showed satisfactory performance, aligning with the results of other studies, in which the SAI for fly ash and metakaolin varied between 80 and 147 % (Donatello et al., 2010b; Donatello et al., 2010a; Tironi et al., 2013; Shafiq et al., 2015; Liu et al., 2017; Siline and Mehsas, 2022). These data place WTPA within this range of acceptable performance.

Fig. 6 shows the correlation between compressive strength tests with lime and Portland cement. Samples WA700, WA800, calcined clay (CC), MK, and FA meet both standards, classifying them as effective pozzolans, while WS100, CL, and LS are deemed unsuitable due to insufficient reactivity. Although the linear equation best represented the results, the correlation was not highly significant.

3.6. R^3

Fig. 7 displays the measurement of combined water content per 100 g of dry paste in mixtures intended for the R^3 test. This technique assesses the pozzolanic reactivity of alternative raw materials by releasing heat and/or chemically combined water (ABNT NM23, 2000; Avet et al.,

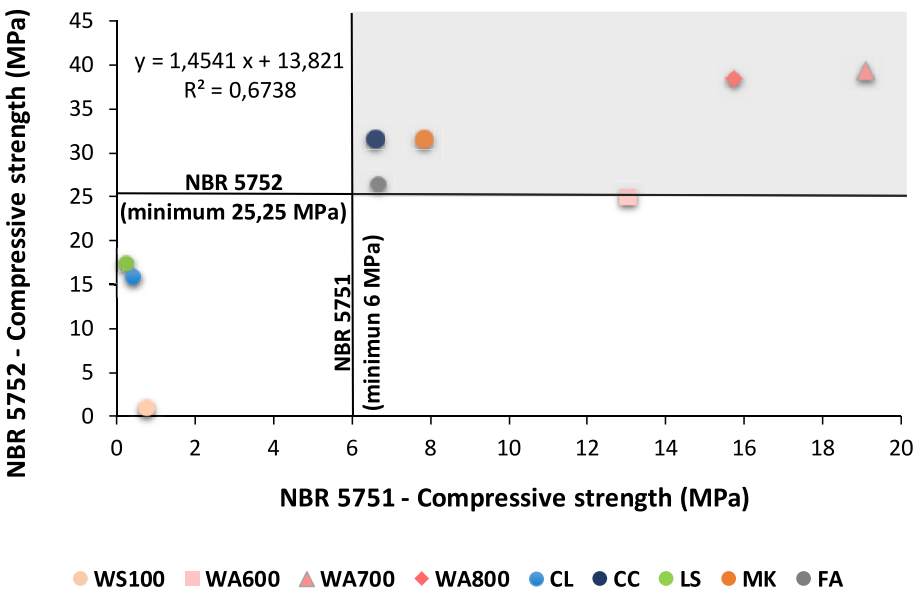

Fig. 6. Correlation of compressive strengths in mortars: Analysis with hydrated lime (based on NBR 5751) versus Portland cement (according to NBR 5752).

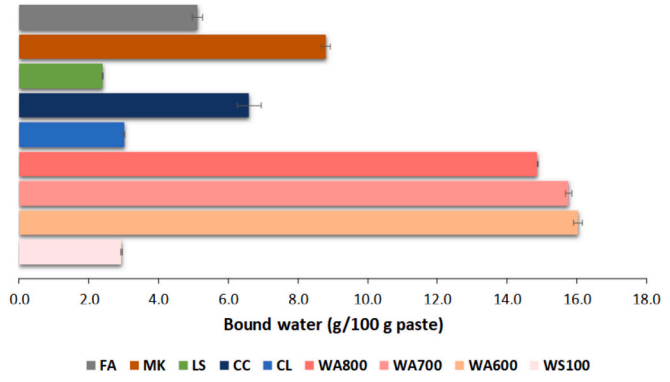

Fig. 7. Characterization of mixtures for R^3 test: mass loss due to combined water with error bars indicating standard deviation from the mean.

2016). The identified water is linked to the dehydration of specific phases such as C-S-H, ettringite, C-A-S-H, and carboaluminates, which are products of exothermic reactions between MCS and $Ca(OH)_2$ (Costa and Pereira Gonçalves, 2021; Ramanathan et al., 2022; Paixão et al., 2023).

At 7 days, MK's chemically combined water content (8.8 g/100 g of paste) exceeded by more than three times the value presented by WS100, CL, and LS, indicating that these systems may be classified as inert. In contrast, the pastes of CC and FA showed levels of chemically combined water between 5 and 6.6 g/100 g, suggesting a moderately pozzolanic categorization for these mixtures. These results are consistent with the discussion presented by Li et al. (2018), who, when analyzing 11 supplementary cementitious materials (SCMs) through a round-robin campaign to investigate 10 different tests, observed that the chemically combined water of fly ash ranged from 3 to 5 g/100 g of paste. The pastes under analysis fall within this upper limit, while the natural pozzolan records 6 g/100 g. This analysis reinforces the pozzolanic nature of the CC and FA systems, comparable to the results observed in previous studies (Liu et al., 2017; Paixão et al., 2023; Pereira et al., 2023).

In the calcined sludge pastes, a slight variation in the content of chemically combined water was observed, ranging between 14.9 and 16.0 g/100 g of paste. Although the WA600 sample did not meet the minimum requirement of 90 % in the SAI, it proved superior to WA800 in the R^3 test, validating its potential as a pozzolan. This can be attributed to the greater chemical availability to react with $Ca(OH)_2$, suggesting a higher degree of reaction in systems processed up to 700 °C. Notably, the chemically combined water in the WTPAs exceeded that of commercial pozzolans, such as FA and MK, approaching double the value for metakaolin.

This variation in the content of chemically combined water reflects the hydrated products formed and is strongly influenced by the composition of the amorphous matrix. The pronounced presence of alumina raises this content, as the hydrates formed (AFt and AFm) contain more constitutional water than those resulting from the silica reaction (Pereira et al., 2023). Thus, the high concentration of kaolinite in the sludge was a determining factor for the greater reactivity observed in the calcined products.

3.7. *Electrical conductivity*

The electrical conductivity method indirectly assesses the pozzolanic potential of materials using an unsaturated calcium hydroxide solution (Paya et al., 2001; Tashima et al., 2014; Basto, 2018). This technique measures the percentage loss of conductivity (% LC) over time, particularly at 100 and 1000 s. Fig. 8 illustrates the conductivity loss curves, which highlight the reductions at these intervals, providing insights into pozzolanic activity.

WTP materials are highly reactive, rapidly consuming hydrated lime and causing a significant %LC increase within seconds. In Fig. 8a, over 50 % of CH is consumed within the first 100 s. The raw WS100 sample exhibited high pozzolanic activity, surpassing calcined samples, consistent with findings by Agra et al. (2023). Carbonaceous particles, as seen in the CL sample, also contribute to conductivity loss, though this is not necessarily linked to pozzolanic reaction.

It is also known that soluble ions, such as Na^+, K^+, and Ca^{2+}, strongly influence the conductivity of a solution by increasing the ionic concentration and, consequently, facilitating electrical conduction (Ogawa et al., 1980; Hewlett and Liska, 2019). At ETA Pirapama, sodium acrylate is used in the coagulation-flocculation process, which may indirectly affect the pozzolanic reactivity in the WS100 sample. This effect is supported Küçükyildirim and Uzal (2014) who observed an increase in conductivity after the addition of zeolites, releasing soluble cations such as sodium, potassium, and calcium. The conductivity of fly ash suspensions in water reflects the concentration and type of ions present, suggesting rapid methods to assess soluble sodium sulfate, potassium,

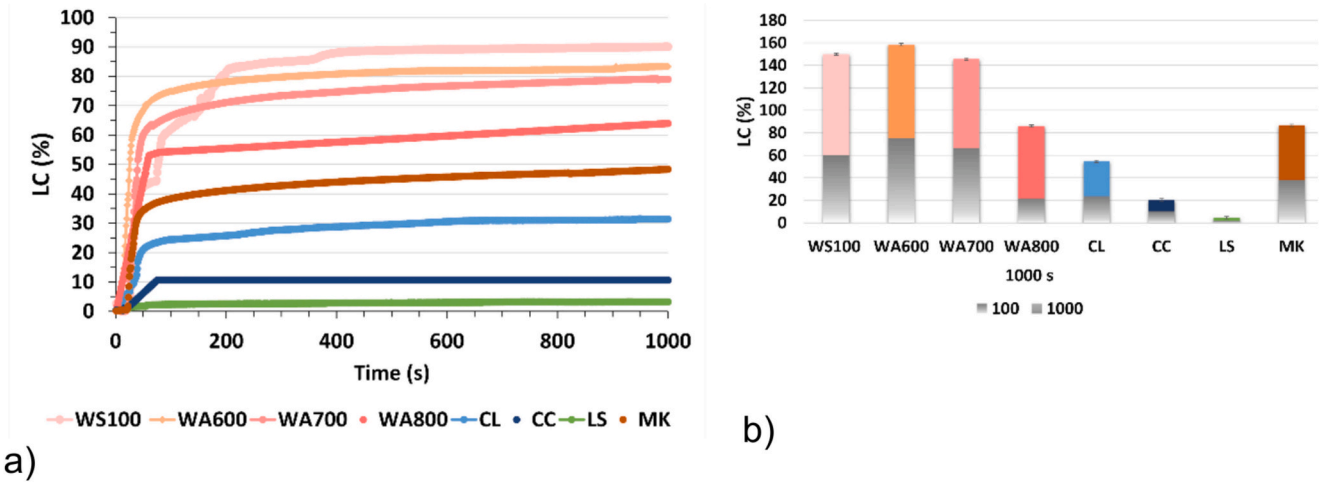

Fig. 8. Conductivity test: a) curve of relative loss of conductivity and b) relative loss in conductivity (%LC) at 100 and 1000 s for water sludge ash calcined at 100 °C, 600 °C, 700 °C, 800 °C, fresh clay, calcined clay, limestone, and metakaolin.

and calcium. These ions typically adhere to fly ash particles as sub-micrometric compounds, significantly influencing their suspension properties (Owens and Waddicor, 1982; Raask, 1982).

LS-water suspensions at 60 °C showed stable conductivity, ranging from 4.96 to 4.91 mS/cm between 100 and 1000 s, as detailed in Table 7. The low %LC of 2.74 % at 1000 s indicates low ion solubility and pozzolanic reactivity, consistent with previous tests.

MK showed a Δ_{1000} of 2.20 mS/cm and $\%LC_{1000}$ of 48.29 %, aligning with literature values of 2.21 to 2.54 mS/cm and 44.51 % to 60.00 % (Velázquez et al., 2014; Fernandes et al., 2017; Basto et al., 2019; Agra et al., 2023). In contrast, WTPA exhibited a Δ_{1000} between 4.47 and 3.39 mS/cm, surpassing metakaolin's conductivity. This highlights WTPA's effectiveness as a pozzolanic material with rapid reaction capabilities compared to traditional pozzolans.

3.8. Response surface design

The experimental results obtained for compressive strength (MPa) and consistency index (CI) are presented in Table 8.

The Response Surface Methodology (RSM) is an essential tool for modeling the relationships between independent variables and one or more dependent variables. Its application enables process optimization and decision-making based on the interaction between such variables and their impacts on the desired response. Through RSM, it is possible to (i) select the most suitable model; (ii) assess data variability through the coefficient of determination (R^2); (iii) calculate the coefficients that structure the model equation; (iv) verify the equation's accuracy with lack-of-fit tests; and (v) optimize and understand the response surface within the experimental context (Myers et al., 1989; Chang et al., 2012). The method employed in this context is Analysis of Variance (ANOVA), as outlined by (Hanrahan and Lu, 2006; Mäkelä, 2017; Zhang et al., 2020).

ANOVA is conducted to examine the model's adequacy and discard variables that do not significantly influence the model (Khan et al., 2016), using tests such as lack-of-fit test (F-test), *t*-test, and R^2. A summary of adjustments for different models is available in Table 9. The suitable models for MPa and IC include linear, interaction, and quadratic terms. The variance analysis results for each model are shown in Table 10.

In RSM, R^2 measures how well the model explains observed variability, but it can increase with more variables, risking overfitting. Adjusted R^2 addresses this by providing a more accurate assessment (Bezerra et al., 2008; Khajeh, 2009; Mahamad et al., 2015). After model selection, *t*-tests evaluate the significance of coefficients (βi) with Ho: βi

Table 7
Electrical conductivity, conductivity variation (Δt), and relative loss conductivity (%LC) for water sludge at 100 °C, 600 °C, 700 °C, 800 °C, fresh clay, calcined clay, limestone, and metakaolin.

Sample	Conductivity (mS/cm)				$(\%LC)_{100}$	$(\%LC)_{1000}$
	$(C_{poza})_{100}$	$(C_{poza})_{1000}$	Δ_{100}	Δ_{1000}		
WS100	1.90	0.48	2.85	4.27	59.99	89.84
WA600	1.34	0.89	4.02	4.47	75.03	83.37
WA700	1.71	1.08	3.41	4.04	66.62	78.96
WA800	4.13	1.87	1.14	3.39	50.65	64.44
CL	4.01	3.61	1.23	1.63	23.49	31.11
CC	4.72	4.72	0.54	0.54	10.21	10.21
LS	4.96	4.91	0.09	0.14	1.83	2.74
MK	2.93	2.45	1.82	2.20	38.30	48.29

Table 8
Experimental results of MPa and IC.

N	Pattern	MPa	IC (mm)
1	"–0"	29.63	197.0
2	"+ − 0"	28.15	321.5
3	"− + 0"	42.53	171.5
4	"++0"	33.37	177.5
5	"-0-"	44.60	150.0
6	"+0-"	41.12	160.5
7	"-0+"	18.36	342.5
8	"+0+"	28.03	379.0
9	"0–"	29.80	244.0
10	"0 + −"	46.53	176.0
11	"0 − +"	19.65	375.0
12	"0++"	29.28	364.0
13	"000"	39.67	299.0
14	"000"	40.70	299.0
15	"000"	37.00	254.0

Table 9
Summary of ANOVA results for the different model types.

Dependent	Model	F-value	P-value	R^2	Adj. R^2	Estimate
MPa	Linear	7.47	0.124	0.7618	0.6968	
	Linear + interactions	7.98	0.116	0.8285	0.6998	
	Quadratic	5.65	0.154	0.9348	0.8174	Suggested
IC	Linear	3.32	0.253	0.7844	0.7256	
	Linear + interactions	3.87	0.22	0.8294	0.7015	
	Quadratic	1.46	0.431	0.9569	0.8792	Suggested

Table 10
ANOVA for the MPa and IC models.

Mpa			IC			
R^2 = 0,9348			R^2 = 0,9569			
Adj R^2 = 0.8174			Adj R^2 = 0.8792			
Lack-of-fit p-value = 0,154			Lack-of-fit p-value = 0,431			
Term	Coefficient	Standard error	P-value	Coefficient	Standard error	P-value
Constant	39.12	2.15	0.000	284.0	16.9	0.000
°C	−0.56	1.31	0.689 (NS)	22.2	10.4	0.085 (NS)
Content	5.56	1.31	0.008	−31.1	10.4	0.030
w/b	−8.34	1.31	0.001	91.2	10.4	0.000
°C*°C	−2.00	1.93	0.349 (NS)	−49.4	15.3	0.023
Content*Content	−3.71	1.93	0.113 (NS)	−17.7	15.3	0.299 (NS)
w/b*w/b	−4.10	1.93	0.087 (NS)	23.4	15.3	0.185 (NS)
°C*Content	−1.92	1.86	0.348 (NS)	−29.6	14.7	0.099 (NS)
°C*w/b	3.29	1.86	0.137 (NS)	6.5	14.7	0.676 (NS)
Content*w/b	−1.78	1.86	0.383 (NS)	14.2	14.7	0.376 (NS)

NS: non-significant (p-value >0.05).

= 0. The T-statistic (|to| = |βi/(standard error βi)|) is compared to the critical value based on significance level α, observations (n), and model parameters (p) (Mäkelä, 2017). Here, α = 0.05 means coefficients with *P* > 0.05 are non-significant (Basaglia and Pietrogrande, 2012; Zhang et al., 2020). The F-test checks for model fit, preferring a non-significant lack of fit, and requires true replications in the experimental design (Pimentel et al., 1996; Bezerra et al., 2008).

3.8.1. Response Surface Model for MPa

Table 10 displays the coefficients of the quadratic model equation, their standard errors, and the P-test values. Notably, the R^2 of 0.9348 is close to the Adj R^2 of 0.8174, indicating a good fit of the model to the experimental data. *P*-values below 0.05 demonstrate the significance of the model terms, with only the water content and w/b ratio showing statistical relevance among the variables. This is expected, as all WTPA exhibited pozzolanic activity independent of the calcination temperature, suggesting that temperature and its interactions do not affect compressive strength. The most significant factor is the water-to-binder ratio, which can be found in the Supplementary Materia, Section 3. Even after removing statistically insignificant terms, they are still considered in the model to provide a comprehensive understanding of the studied system. The final formulation of the second-order response surface for MPa, incorporating all evaluated terms, is expressed by Eq. 6. Fig. 9 presents the contour plot and the three-dimensional representation of the MPa model surface.

$$\begin{aligned}\text{MPa} = {} & 39.12 - 0.56^{\circ}\text{C} + 5.56\ \text{Content} - 8.34\ \text{w/b} - 2.00^{\circ}\text{C}^{*\circ}\text{C} \\ & - 3.71\ \text{Content}^{*}\text{Content} - 4.10\ \text{w/b}^{*}\text{w/b} - 1.92^{\circ}\text{C}^{*}\text{Content} \\ & + 3.29^{\circ}\text{C}^{*}\text{w/b} - 1.78\ \text{Content}^{*}\text{w/b}\end{aligned} \tag{6}$$

Furthermore, the lack of fit test revealed an F value of 5.65, which is lower than the corresponding tabulated value for the degrees of freedom associated with lack of fit and the variances of pure error (19.16), suggesting that there is no evidence of lack of fit with 95 % confidence. In summary, a well-fitted model to the experimental data is characterized by a significant regression and an insignificant lack of fit, indicating that the regression equation explains most of the observed variation. At the same time, the residuals, mainly due to pure errors, represent the remainder. This condition is directly related to the quality of the model (Cornell, 1984; Pimentel et al., 1996). The analysis of residual plots provides additional insights into the model's adequacy, with normal distributions of residuals suggesting a good fit, as evidenced in the Supplementary Material, Section 3. Abnormally large residuals or patterns in the residual plots may indicate the need for adjustments or adding terms to the model (Bruns et al., 2006).

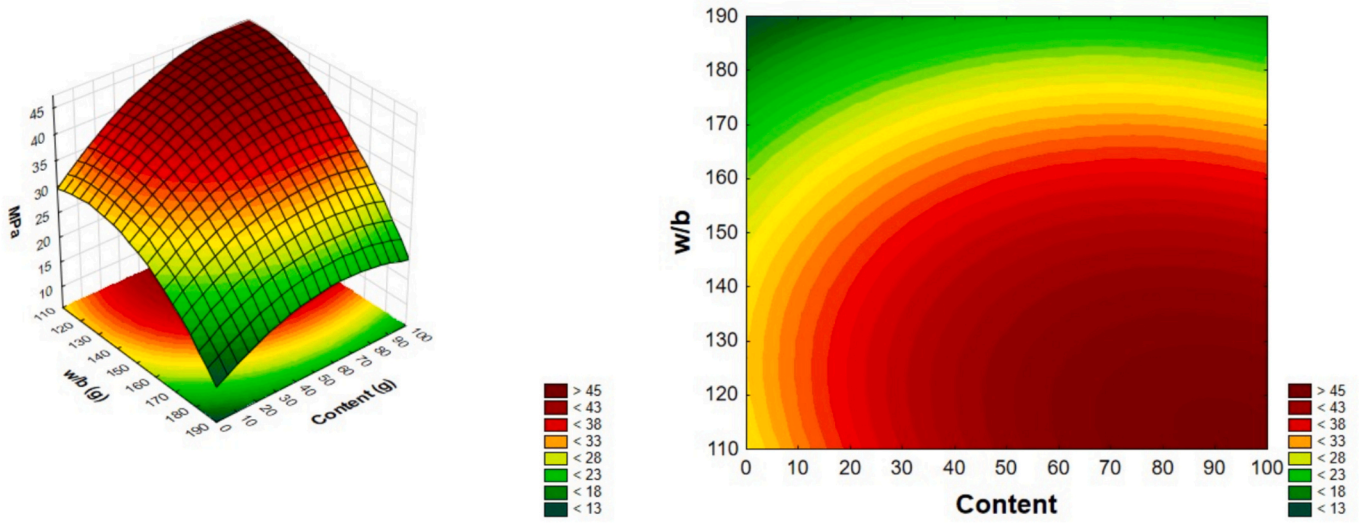

Fig. 9. Response surface of the MPa model (Content vs. a/b, at 700 °C), the graphic axes represent the solid content in the main mixture.

3.8.2. Response Surface Model for IC

The ANOVA of the coefficients for the IC model is presented in Table 10. R^2 and Adj R^2 values are close to 1, indicating a good model. The factors significantly influencing the IC are content, w/b, and °C*°C. Unlike the MPa model, in the IC model, the squared temperature is significant, which is expected, as the different fineness of the materials affects their flowability in the plastic state. Especially the WA600 showed the finest texture and the lowest diametrical index. The derived model for IC at coded levels is given in Eq. 7.

$$\begin{aligned} IC = {} & 284.0 + 22.2^{\circ}C - 31.1\ Content + 91.2\ w/b - 49.4^{\circ}C^{*\circ}C \\ & - 17.7\ Content^{*}Content + 23.4\ w/b^{*}w/b - 29.6^{\circ}C^{*}Content \\ & + 6.5^{\circ}C^{*}w/b + 14.2\ Content^{*}w/b \end{aligned} \quad (7)$$

Compared to Eq. 6 for MPa, the w/b ratio positively influences the mortar consistency (IC), becoming the most relevant factor. On the other hand, the binder content negatively impacts the IC, meaning that the finer the binder, the lower the consistency index, reflecting the adverse effect of the water demand for maintaining workability. The lack of fit test was also used to evaluate the model's adequacy, whose ANOVA results indicated an F value of 1.46. This value is lower than the critical F value from tables, considering the degree of freedom associated with lack of fit and the variance of random error (19.16), thus indicating that there is no evidence of a significant lack of fit at the 95 % confidence level. The representative graphs of the IC model are presented in Fig. 10, offering a graphical visualization of the analysis performed.

3.8.3. Model optimization

The optimization of the model involves setting specific objectives for the desired responses and constraining the variables within an acceptable range or exact values. This allows the model to identify optimal conditions, guiding the search for solutions that meet the established criteria to achieve the best possible performance (Zhang et al., 2020).

As mentioned earlier, the consistency of the mortar directly influences its strength. A too-dry mixture can result in insufficient adhesion and lower strength due to poor distribution of cement and water. In contrast, an overly wet mixture can reduce strength due to excess water, reducing the adequate cement proportion. Moreover, ideal consistency favors effective compaction and minimization of voids, improving strength. Adjustments in water proportion and mortar components are crucial to achieving the consistency for each application, optimizing the final material strength. Therefore, multi-objective optimization should be performed for both MPa and IC models.

The fluidity of the paste is determined by the average of the test results, resulting in a Consistency Index (IC) of 324.41 mm, while the desired compressive strength is 35.57 MPa. After multi-objective optimization, the resulting model is illustrated in the Supplementary Material, Section 3 (where x_1 = temperature in °C, x_2 = content, x_3 = water/cement ratio). The analysis reveals that the ideal combination of LC^3 with WTPA is a temperature of 719.19 °C, 52,86 g of WA700, and 162.42 g of water, equivalent to a 17.62 % cement replacement and a water-to-cement ratio of 0.54, at a temperature of 700 °C.

4. Conclusion

The investigation into the pozzolanic properties of the calcined water treatment sludge revealed that their fineness decreased from 53 to 46.16 m^2/g with the increase in calcination temperature, due to particle sintering, confirmed by laser granulometric analysis, which indicated an increase in the average particle diameter (d_{50} = 28.80 μm). The calcined sludge met the criteria of NBR 12653 for pozzolans, demonstrating good potential, although sintering at 800 °C limited the production of highly reactive materials due to the crystallization of specific phases. The conversion of 70.17 % of kaolinite to metakaolinite, confirmed by XRD analysis, also contributed to the material's reactivity, enhancing its pozzolanic potential. The calcined WTP exhibited significant pozzolanic activity, standing out as a good option for highly reactive pozzolans, especially in lime, SAI, R^3, and electrical conductivity tests, except for the WS100 sample, which showed a false positive in the conductivity test due to the carbonaceous content. In the pozzolanic compressive strength tests with lime, WTPA outperformed commercial pozzolans, with strength exceeding 6 MPa, even at lower calcination temperatures. The WA700 sample showed the best results, while WA600 was limited by fineness and WA800, by sintering, showed lower reactivity. The WS100, CL, and LS samples were inert in the pozzolanicity tests. The R^3 and conductivity tests indicated that the presence of kaolinite in the dry sludge was crucial for the high reactivity of the samples, with WA600 standing out for its higher potential.

The response surface results showed that the ash content and water/cement ratio significantly influence the compression index (IC) and compressive strength (MPa), with the water/cement ratio being the most critical factor. The optimization model identified the ideal configuration for LC^3 mixtures with WTPA, with a calcination temperature of 700 °C, a substitution rate of 17.62 % WTPA, and a water/cement ratio of 0.54. These results suggest that calcined materials, especially WTPA, are promising as highly reactive pozzolans for construction applications.

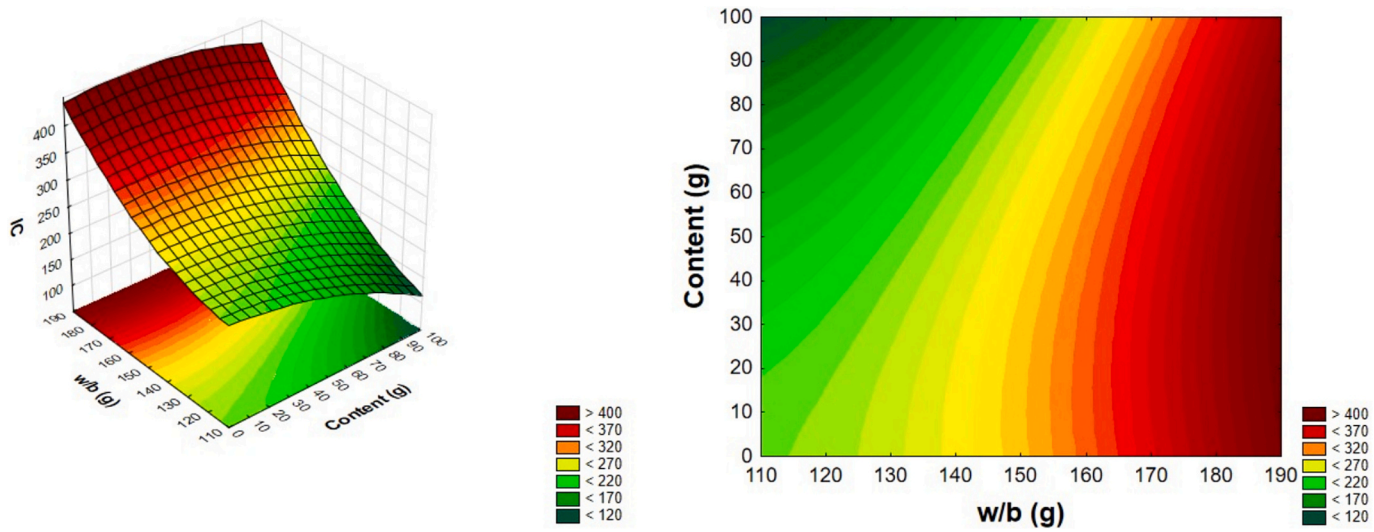

Fig. 10. Response surface of the IC model (Content vs. a/b, at 700 °C), the graphic axes represent the solid content in the main mixture.

CRediT authorship contribution statement

Tacila Bertulino: Writing – review & editing, Writing – original draft, Validation, Software, Resources, Methodology, Investigation, Formal analysis, Data curation, Conceptualization. **Fernanda W.C. Araújo:** Writing – review & editing, Conceptualization. **Antônio A. Melo Neto:** Writing – review & editing, Visualization, Supervision, Resources, Funding acquisition, Conceptualization.

Declaration of competing interest

The authors declare that they have no known competing financial interests or personal relationships that could have appeared to influence the work reported in this paper.

Acknowledgements

The authors acknowledge the financial support provided by the Foundation for Support of Science and Technology of Pernambuco, grant number [IBPG-1375-3.01/20], and thank Compesa, MC-Bauchemie, and Cimento Nacional for providing materials.

Appendix A. Supplementary data

Supplementary data to this article can be found online at https://doi.org/10.1016/j.clay.2025.107741.

Data availability

Data will be made available on request.

References

Abazarpoor, A., Halali, M., 2017. Investigation on the particle size and shape of iron ore pellet feed using ball mill and HPGR grinding methods. Physicochem. Miin. Processing 53, 908–919. https://doi.org/10.5277/ppmp170219.

ABNT NBR 12653, 2014. Pozzolanic materials — Requirements. Brazilian Association of Technical Standards, Rio de Janeiro.

ABNT NBR 13276, 2016. Brazilian Association of Technical Standards. Brazilian Association of Technical Standards, Rio de Janeiro.

ABNT NBR 16372, 2015. Portland Cement and Other Powdery Materials – Determination of Blaine Fineness. Brazilian Association of Technical Standards, Rio de Janeiro, Brazil.

ABNT NBR 5751, 2015. Pozzolanic Materials - Determination of Pozzolanic Activity Wuith Lime at Seven Days. Brazilian Association of Technical Standards, Rio de Janeiro.

ABNT NBR 5752, 2014. Pozzolanic Materials — Determination of the Performance Index with Portland Cement at 28 Days. Brazilian Association of Technical Standards, Rio de Janeiro.

ABNT NBR 7215, 2019. Portland Cement - Determination of Compressive Strength of Cylindrical Specimens. Brazilian Association of Technical Standards, Rio de Janeiro.

ABNT NM23, 2000. Portland Cement and Other Powdered Materials - Determination of Specific Gravity. Brazilian Association of Technical Standards, Rio de Janeiro.

Achon, C.L., Cordeiro, J.S., 2015. Destination and final disposal of sludge generated in WTP - Law 12,305/2010. In: XIX Exhibition of Municipal Experiences in Sanitation, pp. 1–8.

Agra, T.M.S., 2022. Assessment of the Pozzolanicity of Sludge Ash from a Water Treatment Plant (WTP) (Dissertation (Master's)). Federal University of Pernambuco, Recife.

Agra, T.M.S., Lima, V.M.E., Basto, P.E.A., Melo Neto, A.A., 2023. Characterizing and processing a kaolinite-rich water treatment sludge for use as high-reactivity pozzolan in cement manufacturing. Appl. Clay Sci. 236. https://doi.org/10.1016/j.clay.2023.106870.

Ahmad, T., Ahmad, K., Ahad, A., Alam, M., 2016a. Characterization of water treatment sludge and its reuse as coagulant. J. Environ. Manag. 182, 606–611. https://doi.org/10.1016/j.jenvman.2016.08.010.

Ahmad, T., Ahmad, K., Alam, M., 2016b. Sustainable management of water treatment sludge through 3'R' concept. J. Clean. Prod. https://doi.org/10.1016/j.jclepro.2016.02.073.

Ahmad, T., Ahmad, K., Alam, M., 2016c. Characterization of Water Treatment Plant 's Sludge and its Safe Disposal Options. Procedia Environ. Sci. 35, 950–955. https://doi.org/10.1016/j.proenv.2016.07.088.

Alderete, N.M., Villagrán Zaccardi, Y.A., Coelho Dos Santos, G.S., De Belie, N., 2016. Particle size distribution and specific surface area of scm's compared through experimental techniques. In: International RILEM Conference on Materials, Systems and Structures in Civil Engineering Conference Segment on Concrete with Supplementary Cementitious Materials. Technical University of Denmark, Lyngby, Denmark.

Altheman, D., Ferreira, G.C., Montini, M., Gallo, J.B., Rocha, A.I.B.C., 2017. Evaluation of coal fly ash in cementitious matrices. Revista IBRACON de Estruturas e Materiais 10, 1320–1337. https://doi.org/10.1590/s1983-41952017000600009.

Altheman, D., Andréia Gachet, L., Siviero Pires, M., Cristina Cecche Lintz, R., 2023. Water treatment waste as supplementary cementitious material. Mater Today Proc. https://doi.org/10.1016/j.matpr.2023.04.418.

Amaral, M., Macioski, G., de Medeiros, M.H.F., 2021. Pozzolanic activity of silica fume: Analysis in cement pastes with different substitution levels. Revista Materia 26. https://doi.org/10.1590/S1517-707620210003.13023.

Antoni, M., 2013. Investigation of Cement Substitution by Blends of Calcined Clays and Limestone. École Polytechnique Fédérale de Lausanne.

Antoni, M., Rossen, J., Martirena, F., Scrivener, K., 2012. Cement substitution by a combination of metakaolin and limestone. Cem. Concr. Res. 42, 1579–1589. https://doi.org/10.1016/j.cemconres.2012.09.006.

Arikan, M., Sobolev, K., Ertün, T., Yeğinobali, A., Turker, P., 2009. Properties of blended cements with thermally activated kaolin. Constr. Build. Mater. 23, 62–70. https://doi.org/10.1016/j.conbuildmat.2008.02.008.

Arvaniti, E.C., Juenger, M.C.G., Bernal, S.A., Duchesne, J., Courard, L., Leroy, S., Provis, J.L., Klemm, A., De Belie, N., 2015a. Physical characterization methods for supplementary cementitious materials. Mater. Struct. 48, 3675–3686. https://doi.org/10.1617/s11527-014-0430-4.

Arvaniti, E.C., Juenger, M.C.G., Bernal, S.A., Duchesne, J., Courard, L., Leroy, S., Provis, J.L., Klemm, A., De Belie, N., 2015b. Determination of particle size, surface area, and shape of supplementary cementitious materials by different techniques. Mater. Struct. 48, 3687–3701. https://doi.org/10.1617/s11527-014-0431-3.

ASTM C1437, 2020. Standard Test Method for Flow of Hydraulic Cement Mortar. https://doi.org/10.1520/C1437-20.

ASTM C1897–-20, 2000 Standard Test Methods for Measuring the Reactivity of Supplementary Cementitious Materials by Isothermal Calorimetry and Bound Water Measurements. doi:https://doi.org/10.1520/C1437-20.

ASTM C618-19, 2019. Standard Specification for Coal Fly Ash and Raw or Calcined Natural Pozzolan for Use in Concrete. ASTM International, West Conshohocken, PA. https://doi.org/10.1520/C0618-19.

Avet, F.H., 2017. Investigation of the Grade of Calcined Clays Used as Clinker Substitute in Limestone Calcined Clay Cement. École Polytechnique Fédérale de Lausanne.

Avet, F., Scrivener, K., 2018. Investigation of the calcined kaolinite content on the hydration of Limestone Calcined Clay Cement (LC^3). Cem. Concr. Res. 107, 124–135. https://doi.org/10.1016/j.cemconres.2018.02.016.

Avet, F., Snellings, R., Alujas Diaz, A., Ben Haha, M., Scrivener, K., 2016. Development of a new rapid, relevant and reliable (R3) test method to evaluate the pozzolanic reactivity of calcined kaolinitic clays. Cem. Concr. Res. 85, 1–11. https://doi.org/10.1016/j.cemconres.2016.02.015.

Bae, S., Shoda, M., 2005. Statistical optimization of culture conditions for bacterial cellulose production using Box–Behnken design. Biotechnol. Bioeng. 90, 20–28.

Bahman-Zadeh, F., Ramezanianpour, A.A., Zolfagharnasab, A., 2022. Effect of carbonation on chloride binding capacity of limestone calcined clay cement (LC^3) and binary pastes. J. Build. Engi. 52, 104447. https://doi.org/10.1016/j.jobe.2022.104447.

Basaglia, G., Pietrogrande, M.C., 2012. Optimization of a SPME/GC/MS method for the simultaneous determination of pharmaceuticals and personal care products in waters. Chromatographia 75, 361–370. https://doi.org/10.1007/s10337-012-2207-7.

Basto, P.E., 2018. Determination of pozzolanicity by electrical conductivity of wastewater treatment plant (WWTP) sewage sludge as mineral addition to Portland cement (in Portuguese), 99.

Basto, P., Savastano Junior, H., Melo Neto, A.A., 2019. Characterization and pozzolanic properties of sewage sludge ashes (SSA) by electrical conductivity. Cem. Concr. Compos. 104, 103410. https://doi.org/10.1016/j.cemconcomp.2019.103410.

Berenguer, R., Lima, N., Pinto, L., Monteiro, E., Povoas, Y., Oliveira, R., Lima, N.B.D., 2021. Cement-based materials: Pozzolanic activities of mineral additions are compromised by the presence of reactive oxides. J. Build. Engi. 41. https://doi.org/10.1016/j.jobe.2021.102358.

Bezerra, M.A., Santelli, R.E., Oliveira, E.P., Villar, L.S., Escaleira, L.A., 2008. Response surface methodology (RSM) as a tool for optimization in analytical chemistry. Talanta. https://doi.org/10.1016/j.talanta.2008.05.019.

Bishnoi, S., Maity, S., Mallik, A., Joseph, S., Krishnan, S., 2014. Pilot scale manufacture of limestone calcined clay cement : the Indian experience. Ind. Concrete J. 88, 22–28.

Blouch, N., Rashid, K., Zafar, I., Ltifi, M., Ju, M., 2023. Prioritization of low-grade kaolinite and mixed clays for performance evaluation of Limestone Calcined Clay Cement (LC^3): Multi-criteria assessment. Appl. Clay Sci. 243. https://doi.org/10.1016/j.clay.2023.107080.

Bohórquez González, K., Pacheco, E., Guzmán, A., Avila Pereira, Y., Cano Cuadro, H., Valencia, J.A.F., 2020. Use of sludge ash from drinking water treatment plant in hydraulic mortars. Mater Today Commun. 23. https://doi.org/10.1016/j.mtcomm.2020.100930.

Bonavetti, V.L., Rahhal, V.F., Irassar, E.F., 2001. Studies on the carboaluminate formation in limestone filler-blended cements. Cem. Concr. Res. 31, 853–859.

Bonavetti, V.L., Castellano, C.C., Irassar, E.F., 2022. Designing general use cement with calcined illite and limestone filler. Appl. Clay Sci. 230. https://doi.org/10.1016/j.clay.2022.106700.

Box, G.E.P., Hunter, W.G., Hunter, W.S., 1978. Statistics for Experimenters: An Introduction to Design. Data Analysis and Model Building. John Wiley and Sons, New York, NY.

Briki, Y., 2020. 2022. Maximizing the use of supplementary cementitious materials (SCMs) in blended cements.
Bruns, R.E., Scarminio, I.S., Neto, B.N.B., 2006. In: Elsevier (Ed.), Statistical Design-Chemometrics.
BS 3892-1, 1997. Pulverized-Fuel Ash Part 1: Specification for Pulverized-Fuel Ash for Use with Portland Cement. British Standard, London.
Burek, P., Satoh, Y., Fischer, G., Taher Kahil, M., Scherzer, A., Tramberend, S., Fabiola Nava, L., Wada, Y., Wiberg, D., Cosgrove, B., 2016. Water Futures and Solution Fast Track Initiative-Final Report. IIASA.
Cembureau, 2013. The Role of Cement in the 2050 Low Carbon Economy.
Chang, K.-H., Hong, L.J., Wan, H., 2012. Stochastic Trust-Region Response-Surface Method (STRONG)—a New Response-Surface Framework for simulation Optimization. INFORMS J. Comput. 25, 230–243.
Cornell, J.A., 1984. How to Apply Response Surface Methodology. American Society for Quality Control.
Costa, A.R.D., Pereira Gonçalves, J., 2021. Accelerated carbonation of ternary cements containing waste materials. Constr. Build. Mater. 302. https://doi.org/10.1016/j.conbuildmat.2021.124159.
de Carvalho Gomes, S., Zhou, J.L., Li, W., Long, G., 2019. Progress in manufacture and properties of construction materials incorporating water treatment sludge: a review. Resour. Conserv. Recycl. https://doi.org/10.1016/j.resconrec.2019.02.032.
de Oliveira Andrade, J.J., et al., 2018. Performance of rendering mortars containing sludge from water treatment plants as fine recycled aggregate. J. Clean. Prod. 192, 159–168, 10 ago.
de Oliveira Andrade, J.J., Wenzel, M.C., da Rocha, G.H., da Silva, S.R., 2018. Performance of rendering mortars containing sludge from water treatment plants as fine recycled aggregate. J. Clean. Prod. 192, 159–168. https://doi.org/10.1016/j.jclepro.2018.04.246.
Di Bernardo, L., Dantas, A.D.D.B., Voltan, P.E.N., 2012. Métodos e Técnicas de Tratamento e Disposição dos Resíduos Gerados em Estações de Tratamento de Água.
Donatello, S., Freeman-Pask, A., Tyrer, M., Cheeseman, C.R., 2010a. Effect of milling and acid washing on the pozzolanic activity of incinerator sewage sludge ash. Cem. Concr. Compos. 32, 54–61. https://doi.org/10.1016/j.cemconcomp.2009.09.002.
Donatello, S., Tyrer, M., Cheeseman, C.R., 2010b. Comparison of test methods to assess pozzolanic activity. Cem. Concr. Compos. 32, 121–127. https://doi.org/10.1016/j.cemconcomp.2009.10.008.
El Housseini, S., 2022. Hydration and Durability of Fast Hardening Binders Incorporating Supplementary Cementitious Materials (Thèse n° 9930). École Polytechnique Fédérale de Lausanne.
Fernandes, L.F.R., Geraldo, R.H., Saldeira, C.G., Camarini, G., 2017. Evaluation of the Pozzolanic Activity of Porcelain Waste through Electrical Conductivity, in: 1st Workshop on Process Technology and Construction Systems.
Fernandez, R., Martirena, F., Scrivener, K.L., 2011. The origin of the pozzolanic activity of calcined clay minerals: a comparison between kaolinite, illite and montmorillonite. Cem. Concr. Res. 41, 113–122. https://doi.org/10.1016/j.cemconres.2010.09.013.
Filho, J.H., Gobbi, A., Pereira, E., Quarcioni, V.A., De Medeiros, M.H.F., 2017. Atividade pozolânica de adições minerais para cimento portland (Parte i): índice de atividade pozolânica (IAP) com cal, difração de raios-x (DRX), termogravimetria (TG/DTG) e chapelle modificado. Revista Materia 22. https://doi.org/10.1590/S1517-707620170003.0206.
Fontes, C.M.A., Barbosa, M.C., Toledo Filho, R.D., 2003. Potential Use of the Sludge Ash from Sewage Treatment Plants as Supplementary Material in Concretes Production Using Portland Cements (in Portuguese). Federal University of Rio de Janeiro.
Gartner, E., Hirao, H., 2015. A review of alternative approaches to the reduction of CO_2 emissions associated with the manufacture of the binder phase in concrete. Cem. Concr. Res. 78, 126–142. https://doi.org/10.1016/j.cemconres.2015.04.012.
Gastaldini, A.L.G., Hengen, M.F., Gastaldini, M.C.C., Do Amaral, F.D., Antolini, M.B., Coletto, T., 2015. The use of water treatment plant sludge ash as a mineral addition. Constr. Build. Mater. 94, 513–520. https://doi.org/10.1016/j.conbuildmat.2015.07.038.
GCCA - Global Cement and Concrete Association, 2019. Net CO_2 emissions-Weighted average [WWW Document]. https://gccassociation.org/gnr/.
Goldman, A., Bentur, A., 1994. Properties of cementitious systems containing silica fume or nonreactive microfillers. Advn. Cem. Bas. Mat. 209–215.
Grabowski, W., Wilanowicz, J., 2010. Assessment of methods of testing the specific surface of mineral dusts. In: Modern Building Materials, Structures and Techniques, pp. 93–98.
Hagemann, S.E., 2018. Cement-Based Binders, WTP Sludge Ash and Limestone: Influence on Hydration, Compressive Strength and Pore Structure. Universidade Federal de, Santa Maria.
Hagemann, S.E., Gastaldini, A.L.G., Cocco, M., Jahn, S.L., Terra, L.M., 2019. Synergic effects of the substitution of Portland cement for water treatment plant sludge ash and ground limestone: Technical and economic evaluation. J. Clean. Prod. 214, 916–926. https://doi.org/10.1016/j.jclepro.2018.12.324.
Hanrahan, G., Lu, K., 2006. Application of factorial and response surface methodology in modern experimental design and optimization. Crit. Rev. Anal. Chem. 36, 141–151. https://doi.org/10.1080/10408340600969478.
Haustein, E., Kuryłowicz-Cudowska, A., Łuczkiewicz, A., Fudala-Książek, S., Cieślik, B. M., 2022. Influence of Cement Replacement with Sewage Sludge Ash (SSA) on the Heat of Hydration of Cement Mortar. Materials 15. https://doi.org/10.3390/ma15041547.
Heikal, M., El-Didamony, H., Morsy, M., 2000. Limestone-filled pozzolanic cement. Cem. Concr. Res. 30, 1827–1834.
Hendges, L.T., Hendges, L.T., Cristina, R., Reinher, R., Leichtweis, J., Fernandes, É.J., Tones, A.R.M., 2017. Disposição final de lodo de estação de tratamento de água e de esgoto: uma revisão.
Hewlett, P., Liska, M., 2019. Lea's Chemistry of Cement and Concrete. Elsevier Ltda.
Hoppen, C., Portella, K.F., Andreoli, C.V., Sales, A., Joukoski, A., 2005. I-106 - Estudo De Dosagem Para Incorporação Do Lodo De Eta Em Matriz De Concreto, Como Forma De Disposição Final. 23° Congresso Brasileiro de Engenharia Sanitária e Ambiental I-106, pp. 1–9.
Huang, C.H., Wang, S.Y., 2013. Application of water treatment sludge in the manufacturing of lightweight aggregate. Constr. Build. Mater. 43, 174–183. https://doi.org/10.1016/j.conbuildmat.2013.02.016.
IBGE, 2017. National Basic Sanitation Survey 2017: Water Supply and Sanitation. Brazilian Institute of Geography and Statistics.
Januário, G.F., Ferreira Filho, S.S., 2002. Preliminary Environmental Report (RAP) of the exclusive landfill for sludge disposal of the Taiaçupeba WTP. Technical Study. São Paulo 117, 117–126.
Kakali, G., Tsivilis, S., Aggeli, E., Bati, M., 2000. Hydration products of C3A, C3S and Portland cement in the presence of CaCO3. Cem. Concr. Res. 30, 1073–1077. https://doi.org/10.1016/S0008-8846(00)00292-1.
Khajeh, M., 2009. Application of Box-Behnken design in the optimization of a magnetic nanoparticle procedure for zinc determination in analytical samples by inductively coupled plasma optical emission spectrometry. J. Hazard. Mater. 172, 385–389. https://doi.org/10.1016/j.jhazmat.2009.07.025.
Khan, A., Do, J., Kim, D., 2016. Cost effective optimal mix proportioning of high strength self compacting concrete using response surface methodology. Comput. Concr. 17, 629–648. https://doi.org/10.12989/cac.2016.17.5.629.
Koutsouradi, A., Leal da Silva, W.R., Damø, A.J., Jensen, P.A., 2025. Experimental investigation and comparison of soak and flash calcined kaolinite and montmorillonite. Appl. Clay Sci. 265, 107649. https://doi.org/10.1016/j.clay.2024.107649.
Krejcirikova, B., Ottosen, L.M., Kirkelund, G.M., Rode, C., Peuhkuri, R., 2019. Characterization of sewage sludge ash and its effect on moisture physics of mortar. J. Build. Engi. 21, 396–403. https://doi.org/10.1016/j.jobe.2018.10.021.
Küçükyildirim, E., Uzal, B., 2014. Characteristics of calcined natural zeolites for use in high-performance pozzolan blended cements. Constr. Build. Mater. 73, 229–234. https://doi.org/10.1016/j.conbuildmat.2014.09.081.
Lawrence, P., Cyr, M., Ringot, E., 2003. Mineral admixtures in mortars: effect of inert materials on short-term hydration. Cem. Concr. Res. 33, 1939–1947. https://doi.org/10.1016/S0008-8846(03)00183-2.
Li, X., Snellings, R., Antoni, M., Alderete, N.M., Ben Haha, M., Bishnoi, S., Cizer, Ö., Cyr, M., De Weerdt, K., Dhandapani, Y., Duchesne, J., Haufe, J., Hooton, D., Juenger, M., Kamali-Bernard, S., Kramar, S., Marroccoli, M., Joseph, A.M., Parashar, A., Patapy, C., Provis, J.L., Sabio, S., Santhanam, M., Steger, L., Sui, T., Telesca, A., Vollpracht, A., Vargas, F., Walkley, B., Winnefeld, F., Ye, G., Zajac, M., Zhang, S., Scrivener, K.L., 2018. Reactivity tests for supplementary cementitious materials: RILEM TC 267-TRM phase 1. Mater. Struct. 51. https://doi.org/10.1617/s11527-018-1269-x.
Liu, Y., Lei, S., Lin, M., Li, Y., Ye, Z., Fan, Y., 2017. Assessment of pozzolanic activity of calcined coal-series kaolin. Appl. Clay Sci. 143, 159–167. https://doi.org/10.1016/j.clay.2017.03.038.
Liu, J., Zhang, W., Li, Z., Jin, H., Liu, W., Tang, L., 2021. Investigation of using limestone calcined clay cement (LC^3) in engineered cementitious composites: the effect of propylene fibers and the curing system. J. Mater. Res. Technol. 15, 2117–2144. https://doi.org/10.1016/j.jmrt.2021.09.023.
Lothenbach, B., Le Saout, G., Gallucci, E., Scrivener, K., 2008. Influence of limestone on the hydration of Portland cements. Cem. Concr. Res. 38, 848–860. https://doi.org/10.1016/j.cemconres.2008.01.002.
Mahamad, M.N., Zaini, M.A.A., Zakaria, Z.A., 2015. Preparation and characterization of activated carbon from pineapple waste biomass for dye removal. Int. Biodeterior. Biodegradation 102, 274–280. https://doi.org/10.1016/j.ibiod.2015.03.009.
Mäkelä, M., 2017. Experimental design and response surface methodology in energy applications: a tutorial review. Energy Convers. Manag. 151, 630–640. https://doi.org/10.1016/j.enconman.2017.09.021.
Malhotra, V., Mehta, P., 1996. Pozzolanic and Cementitious Materials. Taylor & Francis, Boca Raton, Flórida.
Matschei, T., Lothenbach, B., Glasser, F.P., 2007. The role of calcium carbonate in cement hydration. Cem. Concr. Res. 37, 551–558. https://doi.org/10.1016/j.cemconres.2006.10.013.
Medina, E.A., 2011. Pozolanicidade do metacaulim em sistemas binários com cimento portland e hidróxido de cálcio (Dissertação (Mestrado)). São Paulo.
Monteiro, S.N., Alexandre, J., Margem, J.I., Sánchez, R., Vieira, C.M.F., 2008. Incorporation of sludge waste from water treatment plant into red ceramic. Constr. Build. Mater. 22, 1281–1287. https://doi.org/10.1016/j.conbuildmat.2007.01.013.
Morales, G., 1997. Aproveitamento do lodo de esgoto sanitário como matéria prima para a produção de material pozolânico. Semina: Ciências Exatas e Tecnológicas. 18 (20), 39–45.
Myer, R.H., Montogomery, D.C., 2002. Response Surface Methodology: Process and Product Optimization Using Designed Experiment. John Wiley and Sons, New York.
Myers, R.H., Khuri, A.I., Carter, W.H., 1989. Response Surface Methodology: 1966-1988. Technometrics 31, 137–157.
Nikolov, A., Karamanov, A., 2022. Thermal properties of geopolymer based on fayalite waste from copper production and metakaolin. Materials 15. https://doi.org/10.3390/ma15072666.
Ogawa, K., Uchikawa, H., Takemoto, K., Yasui, I., 1980. The mechanism of the hydration in the system c3s-pozzolana. Cem. Concr. Res. 0, 683–696.

Owaid, H.M., Hamid, R., Taha, M.R., 2014. Influence of thermally activated alum sludge ash on the engineering properties of multiple-blended binders concretes. Constr. Build. Mater. 61, 216–229. https://doi.org/10.1016/j.conbuildmat.2014.03.014.
Owens, P.L.; Waddicor, M.J., 1982. Techniques for the assessment and production control of pulverised fuel ash for use in concrete, in: J.G. Cabrera, A.R.C. (Ed.), International Symposium on the Use of PFA in Concrete. 51–59.
Paixão, R., Carvalho, V.S., Barbosa, L.B., Damasceno Costa, A.R., Pereira Gonçalves, J., 2023. UTILIZAÇÃO DO TESTE RÁPIDO (R^3) PARA AVALIAÇÃO DA REATIVIDADE POZOLÂNICA DO RESÍDUO DE BLOCO CERÂMICO COMO MATERIAL CIMENTÍCIO SUPLEMENTAR. ENARC.
Paya, J., Borrachero, M.V., Monzo, J., Peris-Mora, E., Amahjour, F., 2001. Enhanced conductivity measurement techniques for evaluation of fly ash pozzolanic activity. Cem. Concr. Res. 31, 41–49.
Pereira, V.L.S., Rêgo, J.H., Hoppe Filho, J., 2023. Comparação da reatividade de resíduo de cerâmica vermelha cominuído e matéria-prima de olaria calcinada. Ambiente Construído 23, 255–272. https://doi.org/10.1590/s1678-86212023000400702.
Pimentel, M.F., de Barros, Benício, Neto, B., 1996. Calibração: Uma Revisão para Químicos Analíticos. Quim Nova 19, 268–277.
Pinheiro, B.C.A., Estevão, G.M., Souza, D.P., 2014. Lodo proveniente da estação de tratamento de água do município de Leopoldina, MG, para aproveitamento na indústria de cerâmica vermelha. Parte I: caracterização do lodo. Revista Matéria 19 (3), 451–461. https://doi.org/10.1590/S1517-70762014000300003.
Ptáček, P., Frajkorová, F., Šoukal, F., Opravil, T., 2014. Kinetics and mechanism of three stages of thermal transformation of kaolinite to metakaolinite. Powder Technol. 264, 439–445. https://doi.org/10.1016/j.powtec.2014.05.047.
Raask, E., 1982. Pulverised fuel ash constituents and surface characteristics in concrete applications. In: Cabrera, J.G. (Ed.), Proceedings of the International Symposium on the Use of PFA in Concrete, pp. 5–16.
Ramanathan, S., Tuen, M., Suraneni, P., 2022. Influence of supplementary cementitious material and filler fineness on their reactivity in model systems and cementitious pastes. Mater. Struct. 55. https://doi.org/10.1617/s11527-022-01980-2.
Rashad, A.M., 2013. Metakaolin as cementitious material: history, scours, production and composition-a comprehensive overview. Constr. Build. Mater. https://doi.org/10.1016/j.conbuildmat.2012.12.001.
Ray, S., 2006. S. Ray, RSM: a statistical tool for process optimization. Indian Text. J. 117, 24–30.
Ray, S., Lalman, J.A., 2011. Using the Box-Benkhen design (BBD) to minimize the diameter of electrospun titanium dioxide nanofibers. Chem. Eng. J. 169, 116–125. https://doi.org/10.1016/j.cej.2011.02.061.
Ray, S., Lalman, J.A., Biswas, N., 2009. Using the Box-Benkhen technique to statistically model phenol photocatalytic degradation by titanium dioxide nanoparticles. Chem. Eng. J. 150, 15–24. https://doi.org/10.1016/j.cej.2008.11.039.
Rodríguez, N.H., Ramírez, S.M., Varela, M.T.B., Guillem, M., Puig, J., Larrotcha, E., Flores, J., 2010. Re-use of drinking water treatment plant (DWTP) sludge: Characterization and technological behaviour of cement mortars with atomized sludge additions. Cem. Concr. Res. 40, 778–786. https://doi.org/10.1016/j.cemconres.2009.11.012.
Ruviaro, A.S., Silvestro, L., da Silva Andrade Neto, J., Jean Paul Gleize, P., Pelisser, F., 2023. Eco-efficient cement production: investigating water treatment plant sludge and eggshell filler use in LC^3 systems. Constr. Build. Mater. 394. https://doi.org/10.1016/j.conbuildmat.2023.132300.
Ruviaro, A.S., Silvestro, L., Scolaro, T.P., de Matos, P.R., Pelisser, F., 2021. Use of calcined water treatment plant sludge for sustainable cementitious composites production. J. Clean. Prod. 327. https://doi.org/10.1016/j.jclepro.2021.129484.
Safonov, D., Kinnarinen, T., Häkkinen, A., 2021. An assessment of Blaine's air permeability method to predict the filtration properties of iron ore concentrates. Miner. Eng. 160. https://doi.org/10.1016/j.mineng.2020.106690.
Sales, A., Souza, F.R., Almeida, F.D.C.R., 2011. Mechanical properties of concrete produced with a composite of water treatment sludge and sawdust. Constr. Build. Mater. 25, 2793–2798. https://doi.org/10.1016/j.conbuildmat.2010.12.057.
Sánchez Berriel, S., Favier, A., Rosa Domínguez, E., Sánchez Machado, I.R., Heierli, U., Scrivener, K., Martirena Hernández, F., Habert, G., 2016. Assessing the environmental and economic potential of Limestone Calcined Clay Cement in Cuba. J. Clean. Prod. 124, 361–369. https://doi.org/10.1016/j.jclepro.2016.02.125.
Santos, G.Z.B., Melo Filho, J.A., Pinheiro, M., Manzato, L., 2019. Synthesis of water treatment sludge ash-based geopolymers in an Amazonian context. J. Environ. Manag. 249. https://doi.org/10.1016/j.jenvman.2019.109328.
Schneider, M., Romer, M., Tschudin, M., Bolio, H., 2011. Sustainable cement production-present and future. Cem. Concr. Res. https://doi.org/10.1016/j.cemconres.2011.03.019.
Scrivener, K.L., 2014. Options for the future of cement. Ind. Concrete J. 88, 11–21.
Scrivener, K., Snellings, R., Lothenbach, B., 2016. A Practical Guide to Microstructural Analysis of Cementitious Materials, 1st edition. ed. CRC Press.
Scrivener, K.L., John, V.M., Gartner, E.M., 2018a. Eco-efficient cements: potential economically viable solutions for a low-CO_2 cement-based materials industry. Cem. Concr. Res. 114, 2–26. https://doi.org/10.1016/j.cemconres.2018.03.015.
Scrivener, K., Martirena, F., Bishnoi, S., Maity, S., 2018b. Calcined clay limestone cements (LC^3). Cem. Concr. Res. 114, 49–56. https://doi.org/10.1016/j.cemconres.2017.08.017.
Shafiq, N., Nuruddin, M.F., Khan, S.U., Ayub, T., 2015. Calcined kaolin as cement replacing material and its use in high strength concrete. Constr. Build. Mater. 81, 313–323. https://doi.org/10.1016/j.conbuildmat.2015.02.050.
Shvarzman, A., Kovler, K., Grader, G.S., Shter, G.E., 2003. The effect of dehydroxylation/amorphization degree on pozzolanic activity of kaolinite. Cem. Concr. Res. 33, 405–416. https://doi.org/10.1016/S0008-8846(02)00975-4.
Siline, M., Mehsas, B., 2022. Effect of increasing the Blaine fineness of Metakaolin on its chemical reactivity. J. Build. Engi. 56. https://doi.org/10.1016/j.jobe.2022.104778.
Skibsted, J., Snellings, R., 2019. Reactivity of supplementary cementitious materials (SCMs) in cement blends. Cem. Concr. Res. https://doi.org/10.1016/j.cemconres.2019.105799.
Souri, A., Kazemi-Kamyab, H., Snellings, R., Naghizadeh, R., Golestani-Fard, F., Scrivener, K., 2015. Pozzolanic activity of mechanochemically and thermally activated kaolins in cement. Cem. Concr. Res. 77, 47–59. https://doi.org/10.1016/j.cemconres.2015.04.017.
Tashima, M.M., Soriano, L., Monzó, J., Akasaki, J.L., Payá, J., 2014. New method to assess the pozzolanic reactivity of mineral admixtures by means of pH and electrical conductivity measurements in lime:pozzolan suspensions. Mater. Constr. 64, 316.
Tay, J.-H., Show, K.-Y., 1994. Municipal Wastewater Sludge as Cementitious and Blended Cement Materials. Cem. Concr. Compos. 16, 39–48.
Taylor, H.F.W., 1997. Cement Chemistry, 2 Ed. ed. Thomas Telford, London. https://doi.org/10.1016/s0958-9465(98)00023-7.
Tironi, A., Trezza, M.A., Scian, A.N., Irassar, E.F., 2013. Assessment of pozzolanic activity of different calcined clays. Cem. Concr. Compos. 37, 319–327. https://doi.org/10.1016/j.cemconcomp.2013.01.002.
Velázquez, S., Monzó, J.M., Borrachero, M.V., Payá, J., 2014. Assessment of pozzolanic activity using methods based on the measurement of electrical conductivity of suspensions of Portland cement and pozzolan. Materials 7, 7533–7547. https://doi.org/10.3390/ma7117533.
Yadak Yaraghi, A.H., Ramezanianpour, A.M., Ramezanianpour, A.A., Bahman-Zadeh, F., Zolfagharnasab, A., 2022. Evaluation of test procedures for durability and permeability assessment of concretes containing calcined clay. J. Build. Engi. 58. https://doi.org/10.1016/j.jobe.2022.105016.
Yu, T., Zhang, B., Guo, H., Wang, Q., Liu, D., Chen, J., Yuan, P., 2023a. Calcined nanosized tubular halloysite for the preparation of limestone calcined clay cement (LC^3). Appl. Clay Sci. 232. https://doi.org/10.1016/j.clay.2022.106795.
Yu, T., Zhang, B., Yuan, P., Guo, H., Liu, D., Chen, J., Liu, H., Setti Belaroui, L., 2023b. Optimization of mechanical performance of limestone calcined clay cement: Effects of calcination temperature of nanosized tubular halloysite, gypsum content, and water/binder ratio. Constr. Build. Mater. 389. https://doi.org/10.1016/j.conbuildmat.2023.131709.
Zhang, Q., Feng, X., Chen, X., Lu, K., 2020. Mix design for recycled aggregate pervious concrete based on response surface methodology. Constr. Build. Mater. 259. https://doi.org/10.1016/j.conbuildmat.2020.119776.
Zhang, B., Muhammad, F., Yu, T., Fahimizadeh, M., Hassan, M.A.S., Liang, J., Ning, X., Yuan, P., 2024. Harnessing iron tailings as supplementary cementitious materials in Limestone Calcined Clay Cement (LC^3): an innovative approach towards sustainable construction. Constr. Build. Mater. 453. https://doi.org/10.1016/j.conbuildmat.2024.139111.
Zolfagharnasab, A., Ramezanianpour, A.A., Bahman-Zadeh, F., 2021. Investigating the potential of low-grade calcined clays to produce durable LC^3 binders against chloride ions attack. Constr. Build. Mater. 303. https://doi.org/10.1016/j.conbuildmat.2021.124541.
Zunino, F., Scrivener, K., 2021. Assessing the effect of alkanolamine grinding aids in limestone calcined clay cements hydration. Constr. Build. Mater. 266. https://doi.org/10.1016/j.conbuildmat.2020.121293.